ISSN 2294-4931

IAS

NwLtr 259-260

December 2015

www.sedimentologists.org

International Association of Sedimentologists

IAS Council

Link to **IAS National Correspondents**:
https://www.sedimentologists.org/society/correspondents

CONTENTS

EDITORIAL

Newsletter 259 and 260 have combined in one single issue. The first part reports on the International Travertine- Tufa Workshop was held in Pamukkale University, Geological Engineering Department, Denizli, Turkey and presents some frames of the 31st IAS Meeting of Sedimentology held in Krakow on June 2015.

The central part of the Newsletter is dedicated to Student Grant Reports of the 1st Grant Session 2014. I personally congratulate with the students for the good job done.

Announcement of the 6th International Maar Conference, Jilin University, Nanguan District, Changchun City, Northeast China and the new Student Grant Application guidelines close the Newsletters.

I would like to invite all IAS Members to visit the IAS website and get information on the next 32nd IAS meeting in Marrakech. Note that abstract dead line has been postponed to February 15, 2016

Since Newsletter 256, a new session named «Frames from the World» is launched. Anybody is welcome to contribute to it.

IAS has restyled the webpage (www.sedimentologists.org): please have a look at it, log in and fill the spaces under your profile, and renew your membership for 2015. Remember that being an IAS member gives you the following benefits:

- access to the online versions of Sedimentology and Basin Research, including all issues ever published;
- access to the printed versions of Sedimentology and Basin Research at very favourable rates;
- access to the IAS Member Directory;
- the Friendship Scheme which gives free membership to people in less-developed countries;
- the electronic Newsletter;
- a network of National Correspondents, which report on the activities in their countries;
- International Sedimentological Congress every four years at reduced fees;

- annual Regional Meeting and meetings sponsored by the IAS at reduced fees;
- special lecturer tours allowing sedimentology groups to invite a well-known teacher to give talks and short courses in their country;
- travel grants for PhD student members to attend IAS sponsored meetings;
- research grants for PhD student members (maximum 1.000 Euros);
- institutional grants for capacity building in 'Least Developed Countries' (LDC), (maximum 10.000 Euros)
- biannual Summer Schools focused on cutting edge topics for PhD student members.

I would like to remind all IAS members that:

- the IAS Newsletter 259 is published on-line and is available at: http://www.sedimentologists.org/publications/newsletter
- the next IAS Meeting will be held from 23-25 May 2016 in Marrakech (Morocco). For details, please click: https://www.sedimentologists.org/ims2016

The Electronic Newsletter (ENIAS), started in November 2011, continues to bring monthly information to members. For information on ENIAS contact ias-office@ugent.be

Check the new Announcements and Calendar. Meetings and events shown in **CAPITAL LETTERS** and/or with * are fully or partially sponsored by IAS. For all of these meetings, IAS Student Member travel grants are available. Students can apply through the IAS web site. To receive the travel grant, potential candidates must present the abstract of the sedimentological research they will present at the conference. More info @ www.sedimentologists.org

Vincenzo Pascucci
(IAS General Secretary)

IAS membership for 2016

Dear IAS member,

Thank you for having been a member of IAS in 2015.

In 2015, you were subscribed to receive the **printed version of our journal Sedimentology**. If you wish to **keep receiving Sedimentology in print version also in 2016**, we advise you to **renew your membership now**. The first issue of 2016 (volume 63, issue 1) is now ready to be dispatched. If you renew now, you will be assured of uninterrupted delivery.

Basic membership fees are **25 Euro for full members** and **10 Euro for student members**; add **5 Euro for the printed version** of Sedimentology.

You can **renew your membership for 2016 quickly and safely at the** IAS webpage (after login).

At the same time, please **check (and update if necessary) your personal details and delivery address** to prevent loss of contact or faulty delivery of the printed journals.

We really value your membership... we hope you do so too !

On behalf of the IAS Bureau,
Marc De Batist
Treasurer

REPORT

05-08 NOVEMBER 2015, DENÝZLÝ, TURKEY: TRAVERTINE-TUFA WORKSHOP

INTERNATIONAL TRAVERTINE-TUFA WORKSHOP

On November 05-08, 2015, International Travertine- Tufa Workshop was held in Pamukkale University, Geological Engineering Department, Denizli, Turkey. It has been organized on behalf of **Sedimentology Working Group** and **Pamukkale University, Geological Engineering Department**. The organizing commitee of the Workshop: Mehmet OZKUL (Chairman),

***Figure 1**.- International Travertine-Tufa Workshop Participants in front of conference venue*

Figure 2.- The talk of Prof. Dr. Mehmet Özkul and all participants of the workshop

Ezher TOKER (Secretary), Halil KUMSAR (Member), Samet GUNDUZ (Member), Tamer KORALAY (Member), Arzu GÜL AKÇAY (Member), Kaya TOKER (Member), Barýs SEMIZ (Member), Sefer Beran ÇELIK (Member), Savas TOPAL (Member), Cihan ARATMAN (Member). The scientific committee of the workshop; Atilla Ciner (Istanbul Technical University, Turkey), Baki Varol (Ankara University, Turkey), Enrico Capezzuoli (University of Perugia, Italy), Erdal Kosun (Akdeniz University, Turkey), Erhan Altinel (Eskiºehir Osman Gazi University, Turkey), Esref Atabey (Mineral Research and Exploration General Directorate, Turkey), Ezher Toker (Pamukkale University, Turkey), Faruk Ocakoglu (Eskisehir Osman Gazi University, Turkey), Hükmü Orhan (Selçuk University, Turkey), I. Tonguc Uysal (University of Queensland, Australia), Ýbrahim Turkmen (Balýkesir University, Turkey), Ýsmail Ömer Yýlmaz (Middle East Technical University, Turkey), Mehmet Özkul (Pamukkale University, Turkey), Muhsin Eren (Mersin University, Turkey), Namýk Yalçýn (Ýstanbul University, Turkey), Nizamettin Kazancý (Ankara University, Turkey), Okan Tüysüz (Istanbul Technical University, Turkey), Rudy Swennen (Katholieke Universiteit Leuven, Belgium), Sándor Kele (Macaristan Hungarian Academy of Science, Hungary), Serdar Bayarý (Hacettepe University, Turkey).

The purpose of this

Figure 3.- Participants at the coffee break between sessions.

workshop was to bring together researchers of non-marine carbonates and the students that work in travertine-tufa precipitates. The workshop was attended by nearly 60 registered participants from mainly all different part of the Turkey and also from Italy, Spain, Belgium and Hungary (Fig. 1). There were several good and variable working groups that presented very remarkable results. Master and PhD students were actively involved in presenting talks and posters.

The Travertine-tufa workshop was organized into 2 days of keynotes and some presentations of participitans and 2 days of fieldtrips to Pamukkale, Hierapolis, and Kaklik travertine quarries and Kaklik cave. Participant presented 40 oral and poster contributions.

The presented talks and posters were organized into five thematic sets:

- Travertine
- Tufa and cave deposits
- Isotopes and fluid inclusion applications
- Petrophysical studies on travertine and tufa
- Tectonics, seismicity, palaeoclimate travertine relationship

In addition, the organization was also carried out a Panel on «*The sector of natural stone and Denizli Travertines*».

The sessions were introduced by six excellent keynote lectures given by Li GUO (University of Wales, UK), Concha ARENAS (University of Zaragoza, Spain), Sándor KELE (Institute of Geochemical Research, Hungarian Academy of Sciences, Hungary), Rudy SWENNEN (KU Leuven, Belgium), Ismail Tonguc UYSAL (University of Queensland, Australia) and Erhan ALTUNEL (Eskiºehir Osmangazi University, Turkey).

The first day was organized into two sessions (1 session in the morning and 2 sessions in the afternoon) and 15 poster presentations presented by participants and exhibited during the two days. After the opening talks, Prof. Dr. Mehmet Ozkul gave a thematic presentation titled

Figure 4.- The group photo from the Cocktail at Komurcuoglu Travertine, Koruck town

Figure 5.- The workshop dinner in Yardenbahce, Cankurtaran -Denizli

is «Travel of water to stone: Travertine» (Fig.2). After coffee break, first keynote lecture was given by Li GUO and the title was «*A global spring carbonate GIS database in tectonically active settings*». After lunch break second keynote lecture was «Sedimentology and depositional architecture of fluvial tufa systems» given by Concha Arenas. During the coffee break participants worked through poster presentations and discussed scientific researches (Fig.3).

At the end of the first day, the workshop organized the cocktail at the garden of Kömürcüoðlu Travertine factory and many fantastic sculptures

Figure 6.- All participants were listening to Francesco D'Andria and getting information about Hierapolis

Figure 7.- Hierapolis Antique theater, Pamukkale-Denizli

accompanied with the participants which made by travertine and marbles (Fig.4).

The second day of workshop started with keynote lecture «Stable and clumped isotopes in spring carbonates: enrivonmental and climatic implications» given by Sándor Kele (Hungary) and two more oral presentations related with Isotope and fluid inclusion applications on travertines. After coffee break another significant keynote was given by Rudy Swennen (KU-Leuven, Belgium) about «Travertine as continental carbonate: more then building stone - a study with regard to its reservoir analogue characteristics» at the «Petrophysical studies on travertine and tufa» session.

The end of the second day all participants joined the workshop dinner in Yardenbahce in Cankurtaran, Denizli. The participants were very pleased to taste all different Turkish traditional foods (Fig. 5).

The workshop program was supplemented by two field trips and first day of field trip was dedicated to Hierapolis-Pamukkale. The all participants visited the Hierapolis ancient city and took information from Francesco D'Andria (President of Hierapolis-Pamukkale Archeological Excavation Team) (Fig. 6 &7).

The second stop was Pamukkale and this marvelous place is 20 km north of Denizli city center and located in a seismically and tectonically active zone at the northern margin of the NW trending Denizli Basin that is one of the western Anatolian grabens. The basin is an important region in aspect of travertine precipitation both in Turkey and the world. There are many travertine masses, most of which are inactive, in the region. Pamukkale is the most prominent and famous travertine precipitation site over there. The dazzling white modern travertines are precipitated by warm spring waters of 34 to 58°C rising up along the Pamukkale fault and associated extensional fissures. Therefore, Pamukkale means cotton castle in Turkish.

The last stop of the day was the E–W

Figure 8.- Red water in Karahayit/Pamukkale-Denizli

trending Çukurbað fissure ridge which is ~400 m long, 10 m high and 40 m wide. Past quarrying has exposed the central part of the ridge. Samples from the vertical bands, consisted mostly of calcite and less aragonite that fill the central fissure space yielded U-series ages of ~24.7 to 152 ka. There is another thermal spring named as 'Çukurbað thermal spring' in the southwest foot of the white travertine slope. The thermal spring with temperature of 57°C have higher ionic concentration in comparison with the Pamukkale thermal waters and precipitates red travertine (Fig.8).

The last day of the field trip, the

Figure 9.- Faber quarry in Ballik area, Kaklik, Denizli-Turkey

Figure 10.- Kaklik cave, Denizli-Turkey

participants visited the Kaklik travertine quarries. The first stop was devoted to Ballik area included Faber and Çakmak quarries where is possible to observe the travertine sequences along the quarry walls (Fig. 9). Travertine occurrences evolved from dominantly sub-aqueous, as represented by the sub-horizontal (with conglomerate intercalations) and biostromal reed travertine facies, to dominantly sub-aerial in a thin water film, resulting in the cascade, waterfall and biohermal reed travertine facies.

After lunch the group moved to Kaklik Cave (Fig.10). The visit was enjoyed to see small Pamukkale under the ground. This was the last stop of the field trip and the participants bade farewell to each other.

The occasion is perfect for thanks all people that help us in the organization and success of the International Travertine-Tufa Workshop. Special thanks to Supporting Enterprises (Pamukkale University, Engineering Faculty; Denizli Ticaret Odasi; Denizli Ticaret Borsasi; Enterprise Europe network; EBIC-Ege; Aegean Exporters Associations; Kömürcüoglu Marble Group; Baºaranlar Marble Group, IAS; Geological Engineering Chamber). Financial support from the IAS, particularly in the form of student travel grants for 3 IAS student members from the Hungary (1), Italy (1) and Belgium (1) who actively presented their results as a poster or oral contribution. We are proud to have enjoyed this kind of support. Thanks a lot, IAS!!!

The organization is perfect for thanks all people. The last day of this workshop, the members of Sedimentology Working Group have decided to the next meeting and they announced to the title of the next workshop as «Sedimentology of tectonically active basins». We hope that a new this kind of organization will held in the next edition. Furthermore, it was a great pleasure to have all participants in the International Travertine-Tufa Workshop.

Hope to see you next meetings...

Dr. Ezher TOKER
Secretary of the meeting
IAS National Correspondent of Turkey

FRAMES FROM THE 31ST IAS MEETING OF SEDIMENTOLOGY

The 31st IAS Meeting of Sedimentology was held in Krakow from the 22nd–25th June 2015 under the supervision of the Polish Geological Society, Institute of Geological Sciences, Jagiellonian University in Kraków Institute of Geological Sciences, Polish Academy of Sciences, Faculty of Geology, University of Warsaw and sponsored by International Association of Sedimentologists

The organizing committee composed by:

Michal Gradziñski Chairman (Jagiellonian University in Kraków)
Mariusz Kêdzierski Secretary (Jagiellonian University in Kraków)
Grzegorz Haczewski (Institute of Geological Sciences, Polish Academy of Sciences in Kraków)
Renata Jach Field trip co-ordinator (Jagiellonian University in Kraków)
Piotr Jaglarz Short course coordinator (Jagiellonian University in Kraków)
Artur Kêdzior (Institute of Geological Sciences, Polish Academy of Sciences in Kraków)
Boguslaw Kolodziej (Jagiellonian University in Kraków)
Ewa Malata (Jagiellonian University in Kraków)
Ewa Niesiolowska (Jagiellonian University in Kraków)
Tomasz Rychliñski (Jagiellonian University in Kraków)
Steven De Vriese Webmaster (International Association of Sedimentologists)
Anna Wysocka (University of Warsaw)
Wojciech Wróblewski (Jagiellonian University in Kraków)

Did an enormous effort to make the conference a successful one.

More than 500 people from 50 different countries attended the 31st IAS Meeting.

Twenty-one themes and fifteen Special Session were run during the 3-days conference to present the 1180 communications!! Moreover, four k-notes - Michael D. Blum (Predicting sedimentary system response to human activities: The future of the Mississippi Delta), Brian Jones (Facies and precipitates associated with carbonate-producing hotsprings), Adrian Immenhauser (Mg= Magnesium), and Wojciech Nemec (Colluvium – the ugly duckling of clastic sedimentology) – played indubitably the «main dish» role.

The pictures (by V. Pascucci) record some frames of the conference.

The General Secretary
Vincenzo Pascucci

Figure 1.- Krakow Wavel Castle;

Figure 2.- The dragoon outside the castle;

Figure 3.- People during the A1 Field Trip (Sedimentation on the Serravalian forebulge shelf of the Polish Carpathian Foredeep);

Figure 4.- Map of the Polish Carpathian Foredeep;

Figure 5.- The Chapel of the historic Wieliczka Salt Mine;

Figure 6.- Strange people attending the Gala Dinner in the Wieliczka Salt Mine;

Figure 7.- The IAS President Adrian Immenhauser awards with the Faas Research Prize Richard A. Hale;

Figure 8.- The Organizers of the 31st IAS Meeting of Sedimentology;

Figure 9.- Falling water inside the Wavel Castle.

STUDENT CORNER

Post Graduate Reports

Sedimentary Facies Analysis and Depositional Environment in the Late Quaternary fluvial Successions of Southern Kachchh Mainland, Western India: Climate Vs Tectonic Interplay

Archana Das
PhD Student
Department of Earth and Environmental Science, KSKV Kachchh University, Bhuj, India

Kachchh peninsula in the western India is an excellent example of intraplate seismicity and experiences an arid environment, which provides favourable conditions to investigate the exposed fluvial sequences with ease. The Katrol Hill Fault (KHF) divides the mainland into southern Mainland and northern Mainland. Katrol Hill Range acts as a drainage divide from the northerly and southerly draining streams originate and debouches into the Banni plain and Arabian Sea respectively. In present study we attempted to document the sedimentary facies and depositional environment of exposed sequences of Rukmawati, Nagwanti and Bhukhi rivers (Fig. 1).

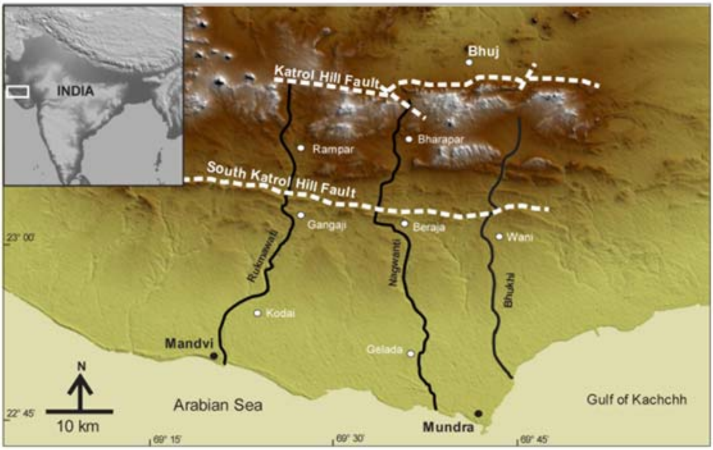

Figure 1: DEM of southern Kachchh Mainland showing main drainages to be studied using IAS support.

Lithostratigraphy and Depositional Environment

We documented sedimentary facies along rivers Rukmawati, Nagwanti and Bhukhi ~ as they spatially cover majority of Southern Kachchh Mainland (SKM). Samples were collected and analyzed for lithofacies analysis and chronology (OSL) study. Precise mapping of sedimentary facies architecture from upstream (source) to downstream (sink) reaches is warranted as it helps reconstruct the depositional environment, Quaternary stratigraphy and palaeohydrological conditions which in turn (aided with chronology) would help evaluate the relative roles of climate and tectonic forcings in evolution of landforms in the SKM (Miall, 1996).

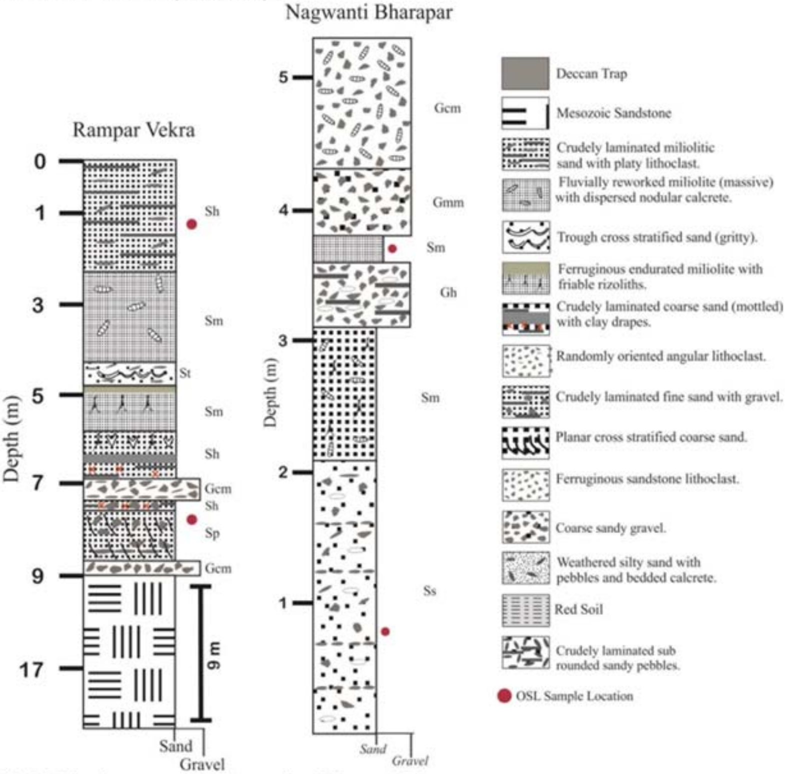

Fig 2: Upland sequences in Rukmawati and Nagwanti Rivers

We studied Rukmawati and Nagwanti rivers in detail and laterally traced the continuity of exposures and facies in Bhukhi river. In all eight sections were studied in detail for their sedimentological attributes namely, facies and depositionsl environment. OSL samples were collected which are been processed and analyzed in OSL laboratory of institute of Seismological Research, India. The sampling and mapping of lithofacies was completed in two field works of two weeks during January 2015 and February 2015.

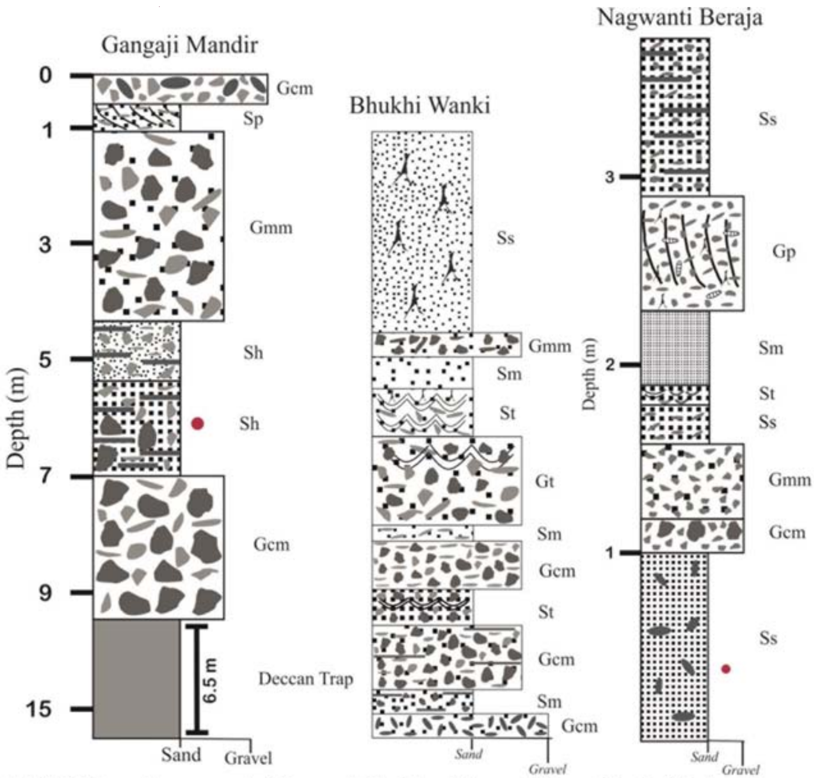

Fig 3: Middle reach sequences in Rukmawati, Bhukhi and Nagwanti Rivers. (See fig 2 for legend)

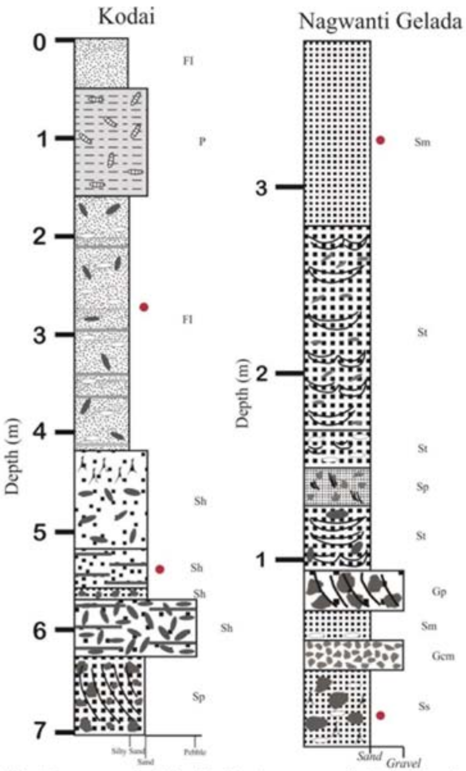

Fig 4: Lower reach (alluvial plains) sequences in Rukmawati and Nagwanti Rivers. (See fig 2 for legend)

OSL Chronology

Samples from freshly exposed sections were collected in stainless steel pipes from five sedimentary units (i.e. unit- 2 and 8 at Rampar Vekra; unit- 2 at Gangaji Mandir and unit- 4 and 6 at Kodai in Rukmawati River. 2 – 3 pipes were collected form each unit so as to increase amount of sample. Samples from both the end of the tube, potentially exposed to daylight during sampling, were removed. Samples were treated with 10% HCl and 30% H_2O_2 to remove the carbonates and the organic matters respectively. Following this, samples were dry sieved to obtain a 90−150 µm size fraction. This fraction was then treated with 40% HF acid for 80 minutes to remove the outer alpha irradiated skin of the quartz grain with continuous stirring and then treated with 12 N HCL for 30 minutes to remove any precipitated fluorides and re-sieved to >90 µm Magnetic grains were removed and pure quartz is extracted by applying a magnetic field of

10,000 gauss using a Frantz Magnetic separator (Model LB1). The etched grains were mounted as a monolayer on stainless steel discs using Silkospray™. Sample purity was checked by infrared stimulation (IRSL) at room temperature. For every sample a minimum of three natural aliquots were used. The samples were considered pure when IRSL to blue-light stimulated luminescence remained <10%. The samples failing the IRSL test were re-etched for 30 minutes by 40% HF. All luminescence measurements were carried out using a RisØ TA-DA-15 reader. The detection optics comprises U-340 and BG-39 filters. Beta irradiations were carried out with 25 mCi ^{90}Sr / ^{90}Y source (radiation dose 7.86±62 Gy/minutes). The elemental concentrations of uranium, thorium and potassium were estimated using the high purity Germanium detector. The cosmic ray estimation is based on the protocol suggested by Prescott and Hutton (1994). (Table-1) In the age calculation, the water content is assumed as 10±2%.

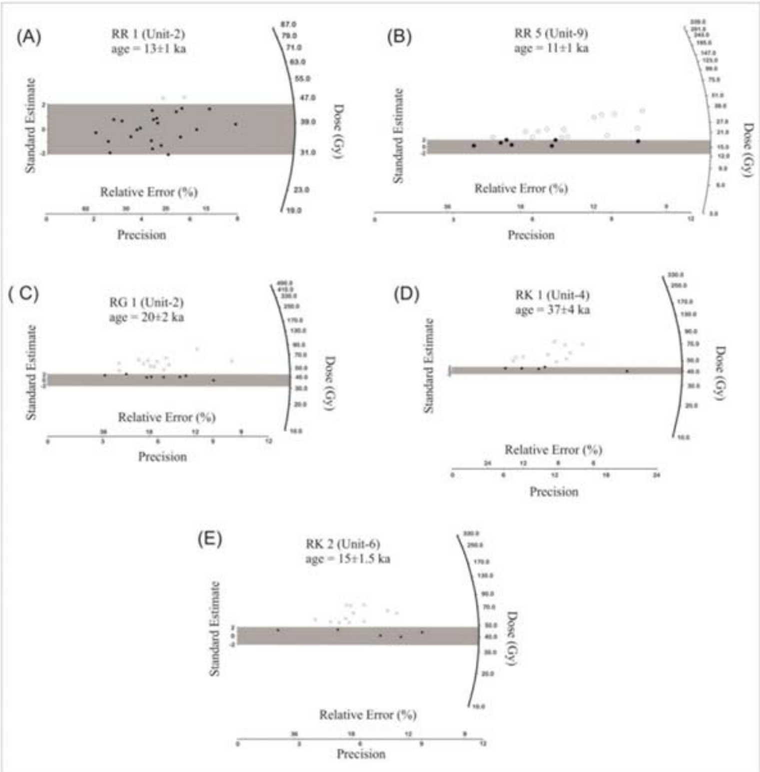

Fig 5: Radial plot of De for Age calculations in Rukmawati River samples.

A conventional Single Aliquot Regeneration (SAR) protocol was used for estimating De (Murray and Wintle, 2000). In SAR protocol, OSL measurement of the natural and regeneration doses (L_x) is divided by OSL response to their respective test doses (T_x). The regenerative doses are chosen in such a way that the corresponding sensitivity-corrected luminescence responses (L_x/ T_x) encompass the natural corrected luminescence (L_n/T_n). De is then obtained through interpolation. A pre heat of 240 degree centigrade for 10 seconds was used whereas the cut heat was 200°C for 0 s.

Typically about 100 aliquots were measured and of these around 20-25 satisfied the criterion of a recycling ratio within 10% of unity. Post-depositional mixing and heterogeneous bleaching due to significant variability in sediment water ratio (discussed above) during the fluvial transport may lead to the presence of more than one dose population (Srivastava et al., 2001). In order to extract the best estimate of the burial dose, statistical models such as the Central Age Model (CAM) of (Galbraith et al., 1999) and the Minimum Age Model (MAM) by Galbraith and Laslett (1993) were employed. In the present study all samples were analyzed using the MAM except for sample RR1 where the over dispersion was <30% CAM was used. Finally radial plots were prepared which to illustrate the precision on the dose estimates (Galbraith et al., 1999) (Fig. 2). At Rampar Vekra, the bottommost unit-2 is dated to 13±1 ka and the unit 8 is dated to 11±1 ka. At Gangaji the lowermost unit-2 is gave an age of 20±2 ka and at Kodai the lowermost unit-4 is dated to 37±4 ka whereas the unit-6 is dated to 15±1.5 ka respectively. Figure 2 gives radial plots of all the samples. Details of radioactivity, dose rate and ages are given in Table 1.

Table 1: Chronometric data for samples of Rukmawati River

Locations	Sample no	U (ppm)	Th (ppm)	K (%)	Cosmic ray dose rate (µGy/a)	Dose rate (µGy/a)	CAM age (ka)	MAM age (ka)
Kodai	Unit 4 (RK 1)	1.05±0.05	6.09±0.3	0.41±0.01	197.7	1256±56	69±5	37±4
Gangaji	Unit 2 (RG 1)	1.49±0.07	10.7±0.5	0.87±0.02	198.4	1900±94	39±3	20±2
Kodai	Unit 6 (RK 2)	2.11±0.1	17.8±0.8	1.08±0.03	197.7	2638±142	29±2	15±1.5
Rampar Vekra	Unit 2 (RR 1)	2.08±0.1	12.9±0.64	1.62±0.05	119±12	2783±113	13±1	7±1
Rampar Vekra	Unit 9 (RR 5)	1.17±0.05	6.46±0.3	0.69±0.02	119±12	1373±54	24±2	11±1

Water content (wt %) = 10 ±2

Additional analysis of rest of the samples is under progress.

Discussion

Dryland Rivers are somehow unique and distinctive as compared to the fluvial environment of perennial rivers. Dryland fluvial system responds sensitively to minor climatic perturbations in an amplified manner. Therefore ephemeral rivers are proficient to carry coarse bed load due to sparse vegetation cover and flashy precipitation caused by localized, convective moisture cells. The present study amalgamates the sedimentological and chronometric data from the fluvial sequences of the Rukmawati river, Nagwanti and Bhukhi basins in the Kachchh region and brings out the chronometric record of the southwest monsoon variability during the 11 ka to 37 ka period. Our study is an input from the extreme western part of India for which the pre - LGM monsoon reconstruction based on fluvial documentation are limited.

Based on preliminary available dates, the oldest sediments are exposed at base of Kodai section, which dates more than 37 ka. Based on facies and regional climatic scenario the period shows enhanced monsoon with fluctuating condition (unit 4) which gradually declining after 37 ka represented by the presence of pebble layer and rhizoliths. Renewed phase of monsoon activity was reported from the Orsang river basin during 60 ka and 30 ka (Juyal et al., 2006) and also reported from the core region of the Thar Desert (Andrews et al, 1998; Jain and Tandon, 2003), Western India (Kale and Rajaguru, 1987) and Central India (Singh et al., 1999; Srivastava et al., 2001). This was followed by fluctuating monsoonal conditions with deposition of clast supported medium to fine sand around 20 ka. The sedimentary characteristics of basal unit (unit 1) in Gangaji which overlying Deccan trap suggests deposition occurred under sediment gravity flow implying onset of dryness which progressively weakened around 20 ka seems most likely as manifestation of LGM period. The sedimentary architecture corresponding to unit 4 to unit 6 in Gangaji suggests that deposition occurred under hyperconcentrated sediment gravity flow with localized channel activity implying weakening monsoon with fluctuations. The gradual improvement in strengthening monsoonal conditions continue as fluvial systems change form braided to meandering stage at around 15 ka. This showed enhanced monsoon with seasonality, leading to floodplain aggradation. This is followed by onset of dryness / declining monsoonal conditions between 15 to 13 ka along with fluctuating monsoonal conditions from humid to dry phases. This period witnessed development of paleosol formation (unit 6 – Kodai section), which is laterally considered 'marker horizon' in Southern Kachchh Mainland. Maurya et al. (2003) dated the pedogenic calcrete using radiocarbon dating as 18980 – 18210 cal. BP and inferred that this paleosol development took place Pre-LGM. However based on our OSL chronology we suggest it to be post LGM (13 ka < pedogenic phase < 15 ka). This was followed by strengthening of monsoonal conditions at < 13ka in form of widespread planar cross stratified sand and is progressively declining during 11 ka. Absence of sediment prior to 13 ka in Rampar indicate that prior to 13 ka, due to the weak ISM (Sirocko, et al., 1993) the hydrological condition were subdued. In dry land fluvial environment, weak monsoon conditions are represented by flashy condition, which might mobilize large volume of sediment from poorly vegetated catchment, but this sediment rarely get preserved in the fluvial record due to infrequent storm surge events. Therefore absence of appreciable sediment pile on the beveled Mesozoic sands stone basement except for the thin angular ferruginous sand stone litho- clasts, suggests that fluvial energy was utilized for the frequent mobilization and lateral planation of the bed rock. Prior to deposition of unit 2 (Rampar) the landscape was experiencing enhanced aridity which gradually strengthened around 13 ka. Considering that in the Khari and Gunawari river preserved sediment till around 3 ka, absence of sediment younger than 11 ka in Rukmawati river could be due to lack of preservation which can be assigned to episodic high intensity rainfall events and or terrain instability caused due to the tectonic activity. At this stage, either of this interpretation would remain speculative till more sequences are studied from the southern Katrol hill range. Therefore, we imply that the incision of the valley-fill sediments and the underlying bedrock occurred during the weak monsoon that began after 11 ka and continued till today.

Conclusion

The oldest sediments are exposed at base of Kodai section, which dates more than 37 ka, indicating the southern Kachchh Mainland alluvial plains at least have archived Late Quaternary sediments. A progressive strengthening of monsoon was observed around 40 ka. This was followed by a decline in monsoon strength around 20 ka manifestation of LGM period. A phase of flood plain aggradation and development of bedded calcrete during 15 ka suggests monsoon with enhanced seasonality. The widespread paleosol formation in southern Mainland Kachchh, which is often used as 'marker horizon; for stratigraphic correlation was formed between 15 ka to 13 ka.

References

1. Andrews, J.E., Singhvi, A.K., Kailath, A.J., Khun, R., Dennis, P.F., Tandon, S.K., Dhir, R.P., 1998. Do stable isotope data from calcrete record Late Pleistocene monsoonal climate variation in the Thar Desert of India? Quaternary Research 50, 240–251.
2. Galbraith, R.F., Roberts, R.G., Laslett, G.M., Yoshida, H., Olley, J.M., 1999. Optical dating of single and multiple grains of quartz from Jinmium Rock Shelter, Northern Australia: part I, experimental design and statistical models. Archaeometry 41, 339 - 364.
3. Huntley, D. J., Godfrey-Smith, D. I. & Thewalt, M. L. W. (1985), Optical dating of sediments. Nature 313, 105–107.
4. Jain, M., Tandon, S.K., 2003. Fluvial response to Late Quaternary climate changes, western India. Quaternary Science Reviews 22, 2223–2235.
5. Juyal, N., Chamyal, L.S., Bhandari, S., Bhushan, R., Singhvi, A.K., 2006. Continental record of the southwest monsoon during the last 130 ka: evidence from the southern margin of the Thar Desert, India. Quaternary Science Reviews 25, 2632 - 2650.
6. Kale, V. S., Rajaguru, S .N., 1987. Late Quaternary alluvial history of the northwestern Deccan upland region. Nature 325, 612–614.
7. Maurya, D.M., Bhandari, S., Thakkar, M.G., Chamyal, L.S., (2003), Late Quaternary fluvial sequences of southern Mainland Kachchh, western India. Current Science 84, 1056–1064.
8. Miall, A. D. **1996**. The Geology of Fluvial Deposits. **Sedimentary Facies**, Basin Analysis, and Petroleum Geology. 582 pp. Berlin, Heidelberg, New York
9. Singh, I.B., Sharma, S., Sharma, M., Srivastava, P., Rajagopalan, G., 1999. Evidence of human occupation and humid climate of 30 ka in the alluvium of southern Ganga Plain. Current Science 76, 1022–1026.
10. Sinha, A., Cannariato, K.G., Stott, L.D., Li, C.H., You, C.F., Cheng, H., Edwards, R.L., Singh, I.B., 2005. Variability of Southwest Indian summer monsoon precipitation during the BØlling-ÅllerØd. Geology 33, 813–816.
11. Sirocko, F., Sarnthein, M., Erlenkeuser, H., Lange, H., Arnold, M., Duplessy, J.C., 1993. Century-scale events in monsoonal climate over the past 24,000 years. Nature 364, 322 – 324.
12. Srivastava, P., Juyal, N., Singhvi, A.K., Wasson, R.J., 2001. Luminescence chronology of river adjustment and incision of Quaternary sediments in the alluvial plains of Sabarmati River, north Gujarat, India. Geomorphology 36, 217–229.
13. Tandon, S.K., Sareen, B.K., Someshwararao, M., Singhvi, A.K., 1997. Aggradation history and luminescence chronology of Late Quaternary semi-arid sequences of the Sabarmati basin, Gujarat, western India. Palaeogeogeography, Palaeoclimatology, Palaeoecology 128, 339–357.

Details of Expenditure (Original Bills Attached)

		INR	Euros
Field visits (32512 + 28876)		61928	**850**
Consumable material for field work / laboratory work		20250	**280**
Travel from Bhuj to Ahmedabad and return with samples		7486	**103**
	Total	**89124**	**1233**

Postgraduate Grant Scheme: Report Cianna E. Wyshnytzky

Minor moraine formation in the Silvrettagletscher, Switzerland foreland

Introduction

This project focuses on series of minor moraines in the high-mountain setting of the Silvrettagletscher, Switzerland foreland (Figure 1). Glaciers are sensitive to climate change, as they are primarily driven by changes in temperature and precipitation over decadal timescales. Some glaciers respond more dynamically to climate change and form "annual" or minor moraines, thus representing the most dynamic end-member response to these changes and hence meriting further attention. To date, most of the studies pertaining to minor moraines focus on lowland settings and only some of these studies employ detailed sedimentological analyses (Andrews and Smithson, 1996; Birnie, 1977; Chandler et al., 2015; Evans and Hiemstra, 2005; Krüger, 1995; Matthews et al., 1995; Reinardy et al., 2013; Sharp, 1984). Most work has assessed the role of climatic mechanisms responsible for minor moraine formation through primarily driving glacial dynamics. Recent work, however, has proposed that the steepness of the ice margin and geometry of the foreland bedrock may be particularly important by affecting insulation, dead-ice incorporation, and differential ablation along the glacier snout (Lukas, 2012).

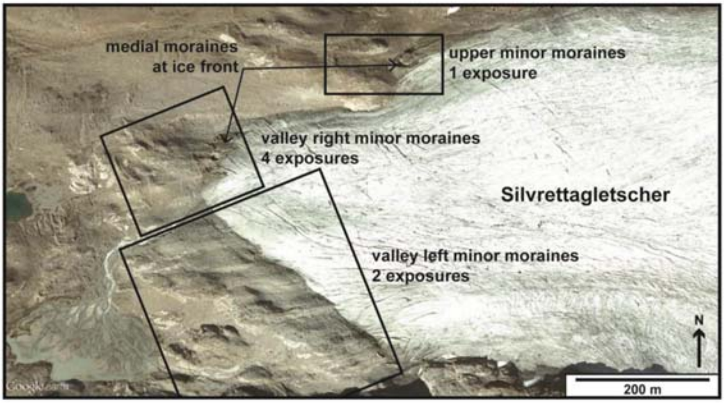

Figure 1. Google Earth image of the Silvrettagletscher, Switzerland foreland, 2010. Boxes and labels denote the three zones that contain minor moraines, with labels and the number of exposures through minor moraines in each area. The two arrows show medial moraines, most prominently emerging at the ice front. The medial moraine towards the western extent of the figure was one feature when this image was collected in 2010 (Geoimage Austria and Google Earth, 2015). This has since split into two separate medial moraines.

Research objectives

The project in the Silvrettagletscher foreland specifically assesses the sedimentology and geomorphology of minor moraines to explain mechanisms of minor moraine formation. This project also compares the positions of minor moraines and other geomorphological landforms to the ice margin through time, to track the evolution of the immediately proglacial foreland.

This project is part of a holistic approach to closing a gap in our understanding of minor moraine formation by focusing on high-mountain settings, here specifically at Silvrettagletscher. This research seeks to establish what the sedimentology and geomorphology of closely spaced minor moraines in this high-mountain environment can reveal about the mechanisms of moraine formation in this setting. The present contribution therefore explores the mechanisms of minor moraine formation related to the physical processes of glacier motion and glaciotectonic deformation of glacial sediments and pre-existing sediments in the foreland. In doing so, this study seeks to compare minor moraine formation in the Silvrettagletscher foreland to processes of minor moraine formation in other settings.

The project at Silvrettagletscher constitutes a smaller part of a larger research project assessing several different field areas in the European Alps. Although sparse, previous work drives the questions of this project. This project seeks to show what the sedimentology and geomorphology of minor moraines can reveal about glacier dynamics and also searches for links between sedimentology and geomorphology among field areas in the Alps and previous global research to help explain the presence of suites of minor moraines in diverse settings.

Methods

This research primarily utilizes sedimentological observations and measurements for the most accurate interpretations of sediment transport and subsequent deposition as moraine landforms. Exposures through minor moraines were manually excavated perpendicular to ridge crests to maintain consistency with inferred ice flow direction. Sedimentological observations and measurements record sedimentary and deformation structures and sedimentary bed and facies architecture. This included measurements of gravel-sized clasts within the exposures, including composition, size, roundness, and form (a-, b-, and c-axes). Similar data were collected from control samples, i.e. where processes of erosion, transport, and deposition are well constrained. This includes subglacial, supraglacial, glaciofluvial, and medial moraine samples.

Geomorphological methods will include tracing the formation and degradation of minor moraines and position of the ice margin through time. This will be accomplished by viewing a suite of glacier measurements (Zemp et al., 2013, 2012), aerial photographs, and remote sensing data.

Preliminary findings

Minor moraines are present in three zones of the Silvrettagletscher foreland. These include: the immediate foreland on valley-left, the immediate foreland on valley-right, and an area on the far valley-right elevated from the primary glaciofluvial system and valley axis due to a prominent bedrock obstruction (Figure 1).

Seven sections were exposed through minor moraines in the Silvrettagletscher foreland. These moraines all contain different sedimentological architectures. The sediment contained within, however, is generally consistent throughout the study area. The moraines contain almost exclusively diamicton and gravel facies. Bedrock constitutes the base of some moraines, and one moraine was composed entirely of sand.

All of the moraines exist on reverse bedrock slopes, echoing the importance of bedrock geometry in minor moraine formation as discussed by Lukas (2012) in the Gornergletscher foreland, providing a similarity between two high-mountain glaciers in the Alps. Additionally, the presence of moraine-like landforms with prominent ice cores was noted throughout the study area (Figure 2), as was also recorded by Lukas (2012). Three prominent medial moraines extending further that the ice front release significant quantities of sediment to the glacier foreland through differential ablation between these insulated debris-covered zones of the glacier and surrounding clean ice. This preliminary work shows the exciting findings that bedrock geometry and the presence of medial moraines primarily influence minor moraine formation in the Silvrettagletscher foreland.

Further work will assess the precise mechanisms of minor moraine formation throughout the foreland. This will include analysis of clast measurements to help determine the source of clasts in the minor moraine exposures, continued compilation of exposed sections into detailed exposure logs and analysis of these logs, and tracing the geomorphological evolution of the foreland through time.

Figure 2. Example of an ice cored moraine. The landform in this photo contains a prominent ice core with sediment draped over both the proximal and distal slopes and sits atop proglacial gravel overlying a reverse bedrock slope. The ridge crest is approximately parallel to the ice front. Similar features were found through the foreland, in all three areas of minor moraines shown on Figure 1. The orientation of these landforms varied, however, where some ridges were parallel to the ice front, some perpendicular, and some somewhere in between. Photo taken in early September 2015, trenching tool for scale.

Acknowledgements

This research benefited immensely from €1000 from the International Association of Sedimentologists Postgraduate Grant Scheme, which partially funded this fieldwork and, therefore, a significant portion of my PhD study. This was used for travel from London to the field area (€100) and room-and-board at the Silvrettahütte (€900).

I have been funded by a Queen Mary University of London Principal's Studentship for my PhD studies. Additional fieldwork funding for the Silvrettagletscher study area includes the QMUL Postgraduate Research Fund, the Royal Geographical Society Dudley Stamp Memorial Award, and the Quaternary Research Association New Research Worker's Award. I am greatly thankful for accommodation and logistical support from the Silvrettahütte.

References cited

Andrews, D.E., Smithson, B.B., 1996. Till fabric of cross valley moraines of north-central Baffin Island, North West Territories, Canada. Geol. Soc. Am. Bull. 77, 271–290.

Birnie, R. V., 1977. A snow-bank push mechanism for the formation of some "annual" moraine ridges. J. Glaciol. 18, 77–85.

Chandler, B.M.P., Evans, D.J.A., Roberts, D.H., 2015. Characteristics of "annual" moraines at a temperate glacier in SE Iceland: insights into patterns, rates and drivers of glacier retreat. Quat. Sci. Rev. (in review).

Evans, D.J. a, Hiemstra, J.F., 2005. Till deposition by glacier submarginal, incremental thickening. Earth Surf. Process. Landforms 30, 1633–1662. doi:10.1002/esp.1224

Geoimage Austria, Google Earth, 2015. (none).

Krüger, J., 1995. Origin, chronology and climatological significance of annual-moraine ridges at Myrdalsjökull, Iceland. The Holocene 5, 420–427.

Lukas, S., 2012. Processes of annual moraine formation at a temperate alpine valley glacier: insights into glacier dynamics and climatic controls. Boreas 41, 463–480. doi:10.1111/j.1502-3885.2011.00241.x

Matthews, J.A., McCarroll, D., Shakesby, R.A., 1995. Contemporary terminal-moraine ridge formation at a temperate glacier: Styggedalsbreen , Jotunheimen, southern Norway. Boreas 24, 129–139.

Reinardy, B.T.I., Leighton, I., Marx, P.J., 2013. Glacier thermal regime linked to processes of annual moraine formation at Midtdalsbreen, southern Norway. Boreas 42, 896–911. doi:10.1111/bor.12008

Sharp, M., 1984. Annual moraine ridges at Skálafellsjökull, south-east Iceland. J. Glaciol. 30, 82–93.

Zemp, M., Frey, H., Gärtner-Roer, I., Nussbaumer, S.U., Hoelzle, M., Paul, F., Haeberli, W., 2012. WGMS (2012): Fluctuations of Glaciers 2005-2010. ICSU (WDS)/ IUGG (IACS)/ UNEP/ UNESCO/ WMO, World Glacier Monit. Serv. Zurich, Switz. X.

Zemp, M., Nussbaumer, S.U., Naegeli, K., Gärtner-Roer, I., Paul, F., Hoelzle, M., Haeberli, W., 2013. WGMS (2013): Glacier Mass Balance Bulletin. ICSU(WDS)/IUGG(IACS)/UNEP/UNESCO/WMO, World Glacier Monit. Serv. Zurich, Switz. 12, 106.

Recrystallization of Middle Triassic dolomites as deduced from petrographic and geochemical trends, Mecsek Mts. and Villány Hills (SW Hungary)

Georgina Lukoczki
PHD student

Supervisors:
Hans G. Machel (University of Alberta, Canada)
Tamás Budai (University of Pécs, Hungary)

Introduction

In the process of dolomitization calcite (calcium carbonate) is transformed to dolomite (calcium-magnesium carbonate). If going to completion, a limestone (rock consisting of >90% calcium carbonate) is transformed to a dolostone (rock consisting of >90% calcium-magnesium carbonate). Dolomitization can happen in multiple ways and geological environments, as represented by a number of models of dolomitization (e.g., critical review by Machel 2004). In almost all of these models Mg is imported to limestone in some type of regional fluid flow, which can be interpreted from the geometry of the dolomite bodies and/or the geochemistry of the dolomites in some cases. However, if the rock is recrystallized, the textures and various geochemical parameters of the dolomites may lead to erroneous genetic interpretations (Machel 1997), i.e., these parameters reflect the process of dolomite recrystallization rather than the process of dolomite formation (= dolomitization). Hence, identification of recrystallization is an essential step in studies attempting to interpret the origin of dolomites and dolostones.

The Middle Triassic Csukma Formation in the Mecsek-Villány area of southwest Hungary (Fig. 1) is suitable to examine dolomitization and recrystallization processes. The Csukma Formation was studied earlier (e.g., Bérczi-Makk et al. 2005 and references therein, Konrád & Budai 2009). However, dolomitization and/or dolomite recrystallization or other diagenetic processes were not investigated in detail.

In my ongoing PhD study, petrographic analysis of 395 stained thin sections from 7 surface outcrops and 6 boreholes identified shallow marine to peritidal depositional environments. The strata were pervasively dolomitized into massive dolostones displaying variable degrees of fabric preservation, ranging from well-preserved depositional fabrics to complete fabric obliteration. Crystal sizes vary from very fine crystalline (crystal diameters ranging from 7 to 26 µm) to coarse crystalline (186 to 395 µm), with planar and non-planar crystal boundaries. Standard petrographic analysis was complemented with cathodoluminescence (CL) petrographic and CL-spectroscopic analysis of 76 thin sections. Seventy-eight samples (64 dolomite and 14 calcite samples of dolostones and dolomite cements, and of limestones and calcite cements, respectively) were analysed for their stable isotopic composition ($\delta^{13}C$, $\delta^{18}O$ ‰). These data complemented with the elemental data obtained during the research activity supported by the IAS Postgraduate Grant Scheme suggest recrystallization and/or multiple events of dolomitization. This report is focussed mainly on the elemental data as they relate to petrography and the stable isotope data.

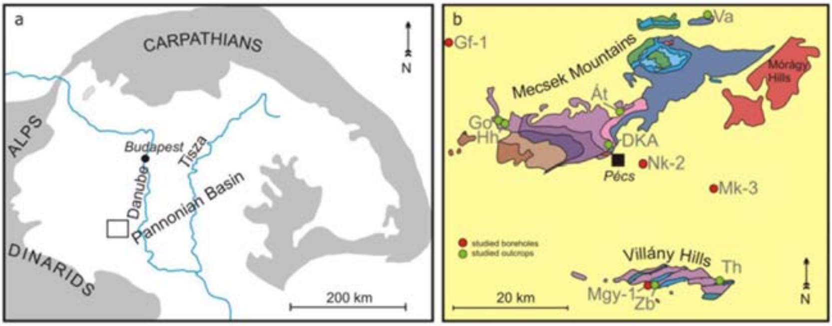

***Figure 1**: (a) Location of the study area in the Pannonian Basin: rectangle south of Budapest. (b) Schematic geological map of the study area showing the sampling locations. Colours refer to geological ages by convention (modified after* BARABÁS *&* KONRÁD *2000).*

Methods

Mean crystal sizes were determined from 40 crystal size measurements on each matrix dolomite and crystalline limestone sample using the QuickPHOTO CAMERA 3.0 Software marketed by CPX-SOLUTIONS by CANIMPEX Enterprises Ltd. The samples were classified based on their average crystal diameters as very fine crystalline (7–26 µm), fine crystalline (37–65 µm), medium crystalline (76–133 µm) and coarse crystalline (186–395 µm) according to natural breaks in the distribution of the crystal sizes, thus intervals somewhat differ from the classification of Folk (1962).

Stable isotope measurements ($\delta^{18}O$, $\delta^{13}C$) were performed in 2013 on micro-drilled calcite and dolomite powder samples at the Institute for Geological and Geochemical Research, Hungarian Academy of Sciences according to the methods of McCrea (1950) and Spötl and Vennemann (2003) on a Finnigan delta plus XP mass spectrometer using international and laboratory standards. Mean values of the measurements are reported relative to Vienna Pee Dee Belemnite standard (V-PDB, ‰). Reproducibility was better than ±0.1‰.

Major, trace and rare earth element concentrations of dolomite and calcite powder samples were measured in the Canadian Centre for Isotopic Microanalysis at the University of Alberta using a Perkin-Elmer Elan 6000 quadrupole Inductively Coupled Plasma – Mass Spectrometer (ICP-MS) in 2014. The samples (~50–100 mg) were dissolved in 8 N HNO_3 (~5 ml) using Savillex beakers and were placed on a hot plate (100 °C) overnight. Solutions were subsequently diluted with 1% HNO_3 to a volume of 90 ml. Prior to ICP-MS analysis, internal standards (In, Bi, and Sc) were added and sample solutions were diluted (with 1% HNO_3) by a factor of 10.

Selected element concentrations were compared to previously obtained stable isotope results and to mean crystal sizes to identify significant and/or insignificant recrystallization as defined by Machel (1997).

Samples

The very fine and fine crystalline samples generally show excellent to fair fabric preservation. The medium–coarse crystalline samples show no or very poor fabric preservation (ghosts of former grains), planar-e, planar-s and non-planar crystal boundaries (*sensu* Sibley and Gregg 1987), and have dull red, mostly mottled CL pattern, often with a narrow zone of limpid dolomite on the inclusion-rich (mottled) cores. One of the selected matrix dolomite samples (coarse crystalline planar-e dolomite, sample Gf-1 926.6 m) is unique inasmuch as the limpid bands around the inclusion-rich cores can be as wide as 70 µm and show distinct zonation. A general trend of increasing $\delta^{18}O$ with increasing crystal size was observed.

One saddle dolomite sample with –15.4‰ $\delta^{18}O$ was selected for later characterization of high temperature dolomitizing fluid.

Two samples of undolomitized limestones were selected for comparative geochemical analysis. These samples are very fine (Át NKF 6) and medium crystalline (DKA-15) limestones with peloid/ooid ghosts (originally ooid/peloid grainstones/packstones?), mottled CL pattern and stable isotope signature of –7.8‰ $\delta^{18}O$ with 1.7‰ $\delta^{13}C$, and –9.0‰ $\delta^{18}O$ with –3.3‰ $\delta^{13}C$, respectively.

Three fracture and/or void filling calcite cement samples with different stable isotopic signatures were selected for the characterization of late diagenetic fluids. Calcite in sample Mk-3 203.0 m is blocky and non-luminescent with –8.3‰ $\delta^{18}O$ and –4.6‰ $\delta^{13}C$, the blocky calcite in sample Nk-2 733.5 m has bright orange luminescence and –14.4‰ $\delta^{18}O$ and -2.1‰ $\delta^{13}C$, whereas the fibrous calcite of the sample Th AKKF 3 is non-luminescent with –7.2‰ $\delta^{18}O$ and –9.1‰ $\delta^{13}C$.

Analytical Results

Results of the elemental analysis are tabulated in Appendix 1 including crystal size and stable isotope data of the analysed samples. Bivariate plots of some of the elemental data vs. crystal size are presented in Appendix 2. The complete data set will be evaluated and integrated at a later time.

Aluminium and potassium

Al and K values were used to discriminate samples with possible clay mineral contamination. Samples with elevated Al and K concentrations (Gf-1 965.8 m and Th P 9) are marked in Appendix 1. Elemental composition of these samples may not be representative of dolomite.

Iron

The Fe concentrations of the matrix dolomites range from 282 ppm to 4624 ppm. Most data falls within the range of 282–1938 ppm with a few outstanding values above 2000 ppm. The highest Fe concentration was found in a very fine crystalline matrix dolomite sample with fairly bright red luminescence (Gf-1 965.8 m), and with high Al and K concentrations, thus, clay contamination is possible, if not likely as the cause for the high Fe value. The coarse crystalline zoned dolomite sample has high Fe content (2357 ppm) relative to the other matrix dolomite samples.

Fe shows a weak negative covariance with crystal size in the case of the medium–coarse crystalline samples: Fe content decreases with increasing crystal size (Fig. 1B, Appendix 2). No such covariance is present (or is negligible) in the case of the very fine and fine crystalline matrix dolomites, and when Fe concentration is compared to $\delta^{18}O$ (Fig. 1A, C, D; Appendix 2).

The Fe content of the saddle dolomite (1643 ppm) falls within the range of the matrix dolomite samples.

The Fe contents of the limestone samples are 440 and 449 ppm and fall within the range of the matrix dolomite samples.

The Fe concentration of two of the three analysed calcite cement samples is low: Mk-3 (203 m) 178 ppm and Th (AKKF 3) 139 ppm, while the third sample, Nk-2 (733.5 m) has relatively high Fe content (1683 ppm).

Manganese

The Mn concentrations of the matrix dolomite samples vary between 15.5 and 149.2 ppm. Most of the data (87.5%) falls within the range of 15.5–77.4 ppm, and consequently Mn concentrations show no/negligible covariance with crystal size and $\delta^{18}O$ (Fig. 2A-D; Appendix 2).

The Mn concentration of the coarse crystalline zoned dolomite is 67.1 ppm. The saddle dolomite cement has the highest Mn concentration (177 ppm) among all analysed dolomite samples.

The Mn concentration of the two limestone samples is 11.1 and 58.4 ppm.

The Mn concentration of the three calcite cement samples differ: it is lowest in the Th AKKF 3 sample (0.68 ppm), medium in the Mk-3 203 m sample (56.5 ppm), and is highest in the Nk-2 733.5 m sample (235 ppm).

Strontium

The Sr values of the matrix dolomites have a relatively narrow range (52–136 ppm) with one outlier (Át ÁGy 4) with significantly higher value (495 ppm) than the other matrix dolomite samples.

A very weak/negligible positive correlation can be observed comparing the Sr content with crystal size and the $\delta^{18}O$ values of the very fine and fine crystalline samples (Fig. 3A, C; Appendix 2. Note: the outlier Át ÁGy 4 sample is removed from the dataset presented in Fig. 3A and C): Sr values increase with increasing crystal size and decreasing $\delta^{18}O$. The same comparison for the medium and coarsely crystalline samples gives a relatively strong negative correlation (Fig. 3B, D; Appendix 2): Sr concentration decreases with increasing crystal size and increasing $\delta^{18}O$ depletion.

The Sr concentrations of the coarse crystalline zoned dolomite and that of the saddle dolomite cement (75.2 ppm and 87.7 ppm, respectively) fall within the range of the Sr values measured on the other dolomite samples.

The limestone sample Át AKF 3 has a similar Sr concentration (417 ppm) to that of the dolomite sample from the same location (Át ÁGy 4: 495 ppm). The Sr content of the limestone sample DKA-15 is 187 ppm.

Sr concentrations of the calcite cements are 16.8 ppm in the Th AKKF 3 sample, 29.6 ppm in the Mk-3 203 m sample, and the highest is in the Nk-2 733.5 m sample (236 ppm).

Sodium

The Na concentrations of the matrix dolomites have a relatively wide range between 43.5–556 ppm. Na has a weak/very weak negative covariance with the crystal size (Fig. 4A, B; Appendix 2). No covariance can be observed in the case of the fine and very fine crystalline matrix dolomites when compared to $\delta^{18}O$ (Fig. 4C; Appendix 2), whereas there is a weak covariance in the case of the medium–coarse crystalline matrix dolomites: Na concentration decreases with increasing $\delta^{18}O$ depletion (Fig. 4D; Appendix 2).

The Na concentrations of the coarse crystalline zoned dolomite (408 ppm) and of the saddle dolomite cement (48.3 ppm) are near the end members of the matrix dolomite values.

Both limestone samples and all calcite cements have low Na concentrations (limestones: Át NKF 6 23.6 ppm; DKA-15 51.9 ppm; calcite cements: Mk-3 203 m 11.2 ppm; Nk-2 733.5 m 11.9 ppm; Th AKKF 3 21 ppm).

Barium

The Ba concentrations of the matrix dolomites range between 0.73 and 7.88 ppm, with most values between 1 and 3 ppm. Comparison of the Ba concentration with the crystal sizes and $\delta^{18}O$ values show negligible covariance (Fig. 5A, C and D; Appendix 2), except in the case of Ba concentration vs. crystal size of the medium–coarse crystalline matrix dolomites. In this case a relatively strong negative covariance can be observed: Ba concentrations decrease with increasing crystal size (Fig. 5B; Appendix 2).

The coarse crystalline zoned dolomite has relatively high Ba content (4.7 ppm), whereas the saddle dolomite cement has a relatively low Ba concentration (1.45 ppm).

Both limestone samples have low Ba concentrations (Át NKF 6 0.58 ppm; DKA-15 0.5 ppm).

The three calcite cement samples are characterized by different Ba concentrations. The lowest Ba concentration was measured in sample Mk-3 203 m (0.92 ppm); the highest in sample Th AKKF 3 (3.98 ppm) with sample Nk-2 733.5 m in between (1.81 ppm).

Rare earth elements

Rare earth elements (REEs) are present in very low concentrations in all analysed samples (dolostones, limestones, saddle dolomite and calcite cements). Sm, Eu, and Dy concentrations are above the detection limit only in 36% of the samples (exclusively matrix dolomites). Where present Sm ranges between 0.1–1.43 ppm. Eu is above the detection limit only in two samples (0.11 and 0.27 ppm). Dy ranges between 0.08 and 1.22 ppm. Tb is below the detection limit in all samples. Ce concentrations are above detection limit in all samples except for one calcite vein (Th AKKF 3). The values range from 0.03 to 15.1 ppm. All highest REE concentrations were measured in the possibly clay contaminated sample (Gf-1 965.8 m).

Lead, cobalt and nickel

The Pb concentrations of all analyzed samples range between 0.31–8.1 ppm (mean=1.63 ppm) with the highest, outstanding value measured on a medium crystalline matrix dolomite sample from the Mecsek (Hh-8/2).

Co concentrations show a narrow range between 1.5–7.2 ppm (mean=4.3 ppm); 71% of the data falls between 3.33 and 4.95 ppm.

Ni concentrations range between 2.5–21.5 ppm (mean=7.2 ppm). The highest, outstanding value was measured on a very fine crystalline matrix dolomite.

Interpretation

Evidence for recrystallization

Geochemical signature of undolomitized limestone samples could be used as a basis for comparison to determine significant recrystallization (*sensu* Machel 1997). However, stable isotopic signatures of the studied limestone samples significantly differ from the values determined for Middle Triassic marine calcites (Korte et al. 2005). Thus, stable isotopic composition of these limestones suggest significant recrystallization with respect to $\delta^{18}O$ and $\delta^{13}C$. Therefore, geochemical signature of these limestone samples cannot be used as basis for comparison. Instead, samples of very fine and fine crystalline dolomites were used as a starting point to determine the degree of recrystallization.

$\delta^{18}O$ values of the studied samples show covariance with crystal size; generally the coarser crystalline the dolomite is, the more depleted it is in $\delta^{18}O$. This trend suggests either dolomitization or recrystallization under increasing temperatures. No covariance can be observed of $\delta^{13}C$ with crystal size. Thus, recrystallization may be significant with respect to $\delta^{18}O$, and insignificant with respect to $\delta^{13}C$.

Trace element analyses of the replacive dolomites can also yield information about the degree of recrystallization. Elements with distribution coefficients (D) less than 1 will be concentrated in the solution during precipitation. Since $D_{Sr}^{dolomite}$, $D_{Na}^{dolomite}$ and $D_{Ba}^{dolomite}$ are <1, successive recrystallization is expected to result in depletion of these elements (Land 1980, and references therein).

The Sr, Na and Ba concentrations of the matrix dolomites show covariance with changes in crystal size and the $\delta^{18}O$: the coarser the dolomite, the more depleted it is $\delta^{18}O$ and in Sr, Na and Ba, which suggests significant recrystallization with respect to Sr, Na and Ba.

Trace elements with distribution coefficients >1 (e.g., Fe, Mn, REEs) will be concentrated in the crystal phase during diagenesis (Veizer 1983), thus, increasing concentration of these elements is expected with increasing crystal size.

Mn, Fe, Co, Ni, Pb, and REE concentrations of the very fine–fine crystalline and medium–coarse crystalline samples falls within the same range with a few outstanding values. Thus, these element concentrations show no or negligible covariance with crystal size and $\delta^{18}O$. Therefore, recrystallization with respect to these elements is deemed insignificant.

Complementing the above trace element results with crystallographic analysis (e.g., Rietveld analysis) is required to better understand the trace element trends and the recrystallization processes of the studied samples.

Cathodoluminescence

Rare earth elements (REEs) can serve as CL activators (e.g., Sm, Tb, Dy, Eu) and sensitizers (e.g., Ce) in carbonates if present in high enough concentration. Pb can also enhance CL. The threshold for activators and sensitizers is 10–20 ppm and 10 ppm, respectively (Machel and Burton 1991). However, none of the samples investigated in this study, except for one probably contaminated by clay minerals, have REEs nor Pb concentrations high enough to cause visible and/or measurable luminescence. This finding is in accordance with the CL spectroscopic observations, Mn being the only element identified on the CL spectra.

Fe, Co and Ni quench CL if present above 30–35 ppm (Machel and Burton 1991). None of the investigated samples have Co or Ni concentrations high enough to quench CL, while Fe concentrations are above the limit to quench CL in all studied samples. Thus, the only elements responsible for the observed CL are Fe and Mn.

Characterization of late diagenetic fluids

Sr of the fine crystalline dolostone and limestone samples from the Central Mecsek (Át ÁGy 4 and Át NKF 6, respectively) show significantly higher concentrations than any other studied samples. These samples were collected in an area where Early Cretaceous sub-volcanic dykes has been found in the vicinity (subsurface and outcrops). Therefore, a hydrothermal/volcanic source of the elevated Sr is possible, suggesting hydrothermal dolomitization and/or alteration at this location. Sub-volcanic dykes were found in the vicinity of other sampling locations as well (Va, Hh) with mostly planar-s and non-planar dolomite textures and well-developed saddle dolomite cements. However, the geochemical signatures of the samples from these location are not distinctive in any way for hydrothermal fluids.

The three studied calcite samples have distinctive geochemical signatures. The bright orange luminescent calcite cement (Nk-2 733.5 m) post-dates the saddle dolomite and has high Fe and Mn concentrations with –14.4‰ $\delta^{18}O$ and –2.1‰ $\delta^{13}C$, indicating a possible basinal origin. The non-luminescent, fibrous calcite (Th AKKF 3) has low Fe and Mn concentrations and a typical meteoric stable isotopic signature. The blocky, non-luminescent calcite sample (Mk-3 203.0 m) has intermediate Fe and Mn concentrations and stable isotopic signature between the basinal and meteoric calcite fluid end-members.

Expenses

ICP-MS measurement of 38 samples in the Canadian Centre for Isotopic Microanalysis at the University of Alberta cost 1400 CAD ≈ 998 EUR (converted from CAD).

Acknowledgements

Financial support from the International Association of Sedimentologists through the Postgraduate Grant Scheme is very much appreciated. The current project was supported by the Doctoral School of Earth Sciences, University of Pécs; "The Developing Competitiveness of Universities in the South Transdanubian Region – SROP-4.2.1.B-10/2/KONV-2010-0002; the Papp Simon Foundation and the Hungarian Scientific Research Fund (OTKA K81296). My research stay at the University of Alberta was supported by the Campus Hungary Scholarship Program. Comments and suggestion of Hans G. Machel on this report, and his supervision of my research activities at the University of Alberta are highly valued.

References

Barabás A., Konrád Gy. 2000 (eds.): Final report on uranium ore exploration in Hungary and on the uranium ore mining in the Western Mecsek Mts. (Manuscript in Hungarian) Mecsekérc Zrt., Pécs, 468 p.

Bérczi-Makk Á. et al. 2004. The Tisza Unit. In Haas J., Budai T., Hips K., Kriványé Horváth Á. (eds.) 2004: Geology of Hungary. Triassic. ELTE Eötvös Kiadó, Budapest, 384 p. (in Hungarian)

Folk, R.L. 1962: Spectral subdivision of Limestone types. In: Ham, W.E. (ed.): Classification of Carbonate Rocks. AAPG Memoir, 1, 62–84.

Konrád Gy., Budai T. 2009: Characteristics of the Middle Triassic sequence of the western Mecsek Mts. Bulletin of the Hungarian Geological Society, 139/2, p. 119–130.

Korte, Ch., Kozur, H.W., Veizer, J. 2005: δ13C and δ18O values of Triassic brachiopods and carbonate rock as proxies for coeval seawater and palaeotemperature. Palaeogeography, Palaeoclimatology, Palaeoecology, 226, pp. 287–306.

Land, L.S. 1980: The isotopic and trace element geochemistry of dolomite: The state of the art. SEPM Spec. Pub., 28, p. 87–110.

McCrea, J.M. 1950: On the isotopic chemistry of carbonates and a paleotemperature scale. Journal of Chemical Physics, 18, 849–857.

Machel, H.G. 1997: Recrystallization versus neomorphism, and the concept of 'significant recrystallization' in dolomite research. Sedimentary Geology, 113, p. 161–168.

Machel, H.G. 2004: Concepts and models of dolomitization: a critical reappraisal. In: Braithwaite, C.J.R., Rizzi, G., and Darke, G. (eds.) The Geometry and Petrogenesis of dolomite hydrocarbon reservoirs. Geological Society, London, Special Publication, 235, p. 7–63.

Machel, H.G., Burton, E.A. 1991: Factors governing cathodoluminescence in calcite and dolomite, and their applications for studies of carbonate diagenesis. In: Barker, C.E, Kopps, O.C. (eds.): Luminescence Microscopy and Spectroscopy: Quantitative and Qualitative Applications, SEPM Short Course Notes 25. p. 37–57.

Sibley, D.F. & Gregg, J.M. 1987. Classification of dolomite rock textures. Journal of Sedimentary Petrology, 57, 967–975.

Spötl, C, Vennemann, T.W. 2003: Continuous-flow isotope ratio mass spectrometric analysis of carbonate minerals. Rapid Communications in Mass Spectrometry, 17, 1004–1006.

Veizer, J. 1983: Chemical diagenesis of carbonates: Theory and application of trace element technique. In: Arthur, M.A., Anderson, Th.F., Kaplan, I.R., Veizer, J., Land, L.S. (eds.): Stable Isotopes in Sedimentary Geology. SEPM Short Course Notes, 10, Chapter 3, 1–100.

Georgina Lukoczki

Sample ID	Location	Description	Crystal size Mean (µm)	σ	Stable isotopes $\delta^{18}O$ (‰ PDB)	$\delta^{13}C$	Analyzed elements (ppm) Na	Al	K	Mn	Fe	Co	Ni	Sr	Ba	Ce	Sm	Eu	Tb	Dy	Pb
						DL	0.5	0.2	6	0.03	3.7	0.03	0.06	0.03	0.03	0.03	0.04	0.03	0.03	0.04	0.03
Gf-1 1055.0 m	Mecsek	very fine crystalline matrix dolomite	17	3	-4.1	2.1	362	724	614	35.5	1601	4.44	21.5	77.4	2.36	1.57	0.14	<DL	<DL	0.15	0.75
Gf-1 1109.0 m	Mecsek	very fine crystalline matrix dolomite	13	4	-2.8	2.4	556	1863	1688	65.9	2307	4.99	4.89	109	5.43	2.48	0.27	<DL	<DL	0.24	2.17
Gf-1 965.8 m	Mecsek	very fine crystalline matrix dolomite	23	8	-3.4	1.9	408	2969	3144	149	4624	6.18	6.58	99.8	7.81	15.1	1.43	0.27	<DL	1.22	5.29
Gf-1 982.0 m	Mecsek	very fine crystalline matrix dolomite	16	5	-3.9	2.6	303	266	238	37.8	986	4.66	5.29	97.3	1.88	0.93	<DL	<DL	<DL	0.11	1.05
Gf-1 992.0 m	Mecsek	very fine crystalline matrix dolomite	16	5	-4.5	1.9	497	666	496	28.3	1267	4.23	11.5	89.9	2.06	1.37	0.12	<DL	<DL	0.12	0.62
Gf-1 998.0 m	Mecsek	very fine crystalline matrix dolomite	14	3	-4.0	1.7	434	624	455	30.3	1160	4.18	2.48	103	2.01	2.46	0.25	<DL	<DL	0.23	1.03
Go-3/1	Mecsek	very fine crystalline matrix dolomite	26	7	-3.2	1.9	212	458	294	33.5	1558	1.51	8.75	59.2	1.34	1.02	<DL	<DL	<DL	<DL	0.46
Hh-26	Mecsek	very fine crystalline matrix dolomite	17	4	-3.5	2.5	151	898	333	27.8	874	2.75	4.86	63.6	3.45	3.03	0.30	<DL	<DL	0.22	1.57
Mgy-1 253.8 m	Villány	very fine crystalline matrix dolomite	22	5	-1.1	2.2	369	485	269	17.4	520	3.96	11.0	103	1.35	0.63	<DL	<DL	<DL	0.09	0.90
Mgy-1 339.7 m	Villány	very fine crystalline matrix dolomite	20	4	-2.1	1.7	186	813	474	38.2	637	4.32	3.58	75.5	2.47	1.15	0.12	<DL	<DL	0.11	0.85
Mgy-1 346.9 m	Villány	very fine crystalline matrix dolomite	16	4	-1.6	1.7	244	823	481	38.3	702	3.83	4.81	84.0	2.64	1.42	0.17	<DL	<DL	0.19	0.71
Mk-3 182.6 m	Villány	very fine crystalline matrix dolomite	11	3	-1.8	1.2	298	420	175	59.5	750	3.33	5.42	83.5	2.90	1.06	0.10	<DL	<DL	0.10	1.09
Nk-2 709.0 m	Villány	very fine crystalline matrix dolomite	11	2	-3.0	1.4	154	1129	477	80.8	1938	4.52	12.6	72.5	5.13	3.82	0.37	<DL	<DL	0.35	1.14
Th Ép 4	Villány	very fine crystalline matrix dolomite	7	2	-3.4	-0.7	343	1545	668	72.5	1212	3.47	3.37	88.5	2.49	2.97	0.29	<DL	<DL	0.24	1.82
Th P 9	Villány	very fine crystalline matrix dolomite	20	5	-0.5	0.8	240	3870	2503	97.8	2927	4.73	5.40	73.7	6.13	6.11	0.58	0.11	<DL	0.44	3.42
Zb-4	Villány	very fine crystalline matrix dolomite	24	6	-1.5	2.3	177	307	115	20.4	396	3.43	2.62	74.5	1.82	0.87	<DL	<DL	<DL	0.12	0.43
Zb-6	Villány	very fine crystalline matrix dolomite	26	6	-2.3	1.5	137	143	55	19.5	282	3.59	2.58	64.0	1.13	0.35	<DL	<DL	<DL	0.09	0.45
Át ÁGy 4	Mecsek	fine crystalline matrix dolomite	64	21	-10.2	1.9	228	850	610	30.7	1766	4.14	9.04	495	3.92	1.62	0.44	<DL	<DL	0.41	1.17
Gf-1 954.6 m	Mecsek	fine crystalline matrix dolomite	57	14	-8.4	2.3	163	988	902	61.3	1726	4.44	11.6	106	1.99	1.41	0.16	<DL	<DL	0.15	1.92
Mgy- 1 170.4 m	Villány	fine crystalline matrix dolomite	38	9	-3.2	1.0	212	375	187	38.1	408	3.98	6.12	97.3	1.24	0.55	<DL	<DL	<DL	0.08	0.60
Mgy-1 342.3 m	Villány	fine crystalline matrix dolomite	50	14	-3.8	2.2	111	237	106	52.5	447	3.92	6.51	66.2	0.73	0.34	<DL	<DL	<DL	<DL	0.90
Mgy-1 366.5 m	Villány	fine crystalline matrix dolomite	37	10	-2.6	2.0	188	372	159	47.8	519	4.22	10.4	77.2	1.25	0.41	<DL	<DL	<DL	0.11	0.74
Mgy-1 374.5 m	Villány	fine crystalline matrix dolomite	65	17	-3.6	1.5	239	464	228	54.7	491	4.32	11.4	111	1.97	1.35	0.25	<DL	<DL	0.25	1.23
Mgy-1 381.5 m	Villány	fine crystalline matrix dolomite	51	15	-3.8	1.6	145	223	92	25.3	332	3.70	8.49	88.1	1.18	0.56	0.10	<DL	<DL	0.14	0.70
Gf-1 918.2 m	Mecsek	medium crystalline matrix dolomite	76	23	-6.7	2.4	246	1624	1691	61.0	1788	4.80	5.37	108	3.45	2.87	0.32	<DL	<DL	0.21	2.00
Hh-8/2	Mecsek	medium crystalline matrix dolomite	133	44	-12.5	2.1	43.5	633	172	37.1	1234	2.32	10.4	52.5	2.18	3.56	0.36	<DL	<DL	0.30	8.10
Va 3T/1	Mecsek	medium crystalline matrix dolomite	186	62	-7.5	2.4	306	281	152	104	1047	3.63	3.60	75.1	1.76	0.49	<DL	<DL	<DL	0.09	1.33
Mgy-1 318.7 m	Villány	medium crystalline matrix dolomite	85	20	-4.4	-0.3	185	531	258	77.4	622	4.95	5.16	136	1.56	1.79	0.21	<DL	<DL	0.21	3.76
Mgy-1 333.5 m	Villány	medium crystalline matrix dolomite	99	21	-4.0	-0.1	209	956	569	39.3	1011	3.74	3.71	126	2.80	2.21	0.22	<DL	<DL	0.17	1.46
Gf-1 926.6 m	Mecsek	coarse crystalline matrix dolomite	395	75	-8.0	2.2	408	1336	1577	67.1	2357	4.36	4.36	75.2	4.70	5.26	0.55	<DL	<DL	0.38	1.02
Hh-4	Mecsek	coarse crystalline matrix dolomite	210	88	-6.3	3.0	113	76.1	22	53.0	1020	2.15	5.34	57.8	1.55	0.46	<DL	<DL	<DL	<DL	2.14
Mk-3 329.7 m b	Villány	coarse crystalline matrix dolomite	217	62	-7.1	0.4	68.3	135	30	15.5	432	3.02	8.75	62.3	1.53	0.46	<DL	<DL	<DL	<DL	1.30
Va 3T/2	Mecsek	saddle dolomite cement			-15.4	1.1	48.3	539	13	177	1643	3.95	9.94	87.7	1.45	0.26	<DL	<DL	<DL	<DL	4.52
Át NKF 6	Mecsek	very fine crystalline limestone	25	7	-7.8	1.7	23.6	43.8	39	11.1	440	6.64	5.77	417	0.58	0.33	<DL	<DL	<DL	<DL	1.09
DKA-15	Mecsek	medium crystalline limestone	176	44	-9.0	-3.3	51.9	53.8	57	58.4	449	6.91	4.10	187	0.50	0.41	<DL	<DL	<DL	<DL	1.75
Mk-3 203.0 m a	Villány	calcite cement			-8.3	-4.6	11.2	54.3	54	56.5	178	7.21	5.97	29.6	0.92	0.22	<DL	<DL	<DL	<DL	0.31
Nk-2 733.5 m	Villány	calcite cement			-14.4	-2.1	11.9	4.7	1	235	1683	5.94	9.47	236	1.81	0.03	<DL	<DL	<DL	<DL	1.33
Th AKKF 3	Villány	calcite cement			-7.2	-9.1	21.0	19.7	17	0.68	139	6.53	10.1	16.8	3.98	<DL	<DL	<DL	<DL	<DL	0.81

samples with eleveted Al and K concentrations

I

Appendix 1

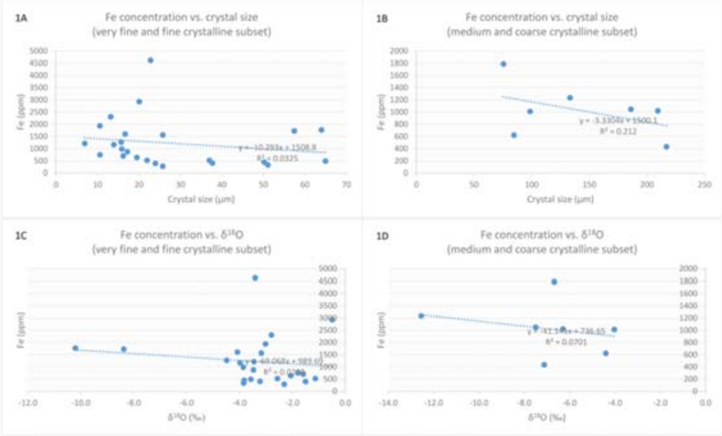
1A
Fe concentration vs. crystal size
(very fine and fine crystalline subset)
Fe (ppm)
Crystal size (µm)
1B
Fe concentration vs. crystal size
(medium and coarse crystalline subset)
Fe (ppm)
Crystal size (µm)
1C
Fe concentration vs. δ18O
(very fine and fine crystalline subset)
Fe (ppm)
δ18O (‰)
1D
Fe concentration vs. δ18O
(medium and coarse crystalline subset)
Fe (ppm)
δ18O (‰)

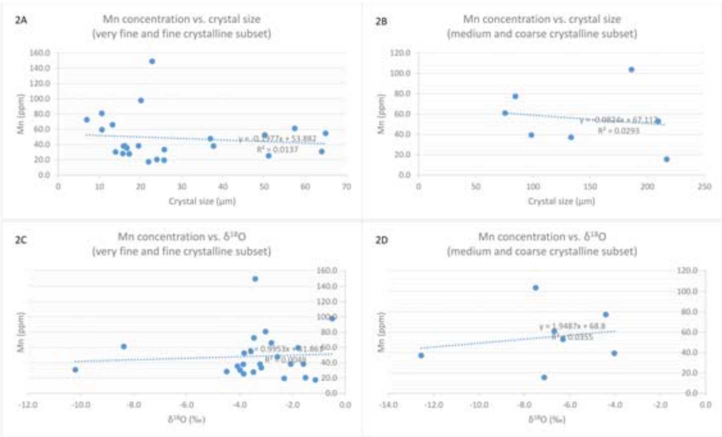
2A
Mn concentration vs. crystal size
(very fine and fine crystalline subset)
Mn (ppm)
Crystal size (µm)
2B
Mn concentration vs. crystal size
(medium and coarse crystalline subset)
Mn (ppm)
Crystal size (µm)
2C
Mn concentration vs. δ18O
(very fine and fine crystalline subset)
Mn (ppm)
δ18O (‰)
2D
Mn concentration vs. δ18O
(medium and coarse crystalline subset)
Mn (ppm)
δ18O (‰)

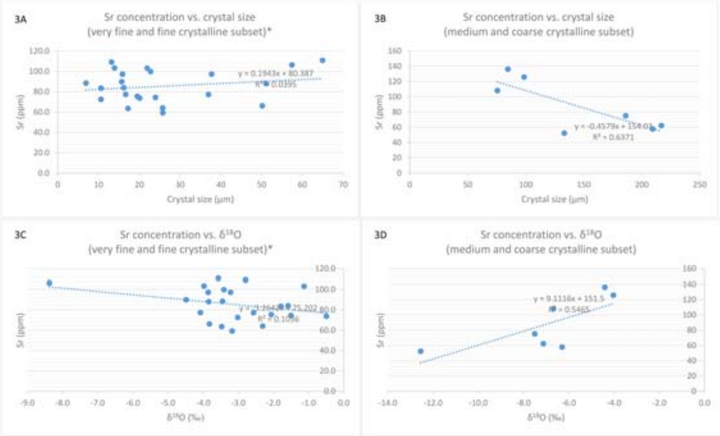

*without sample Át Ágy 4

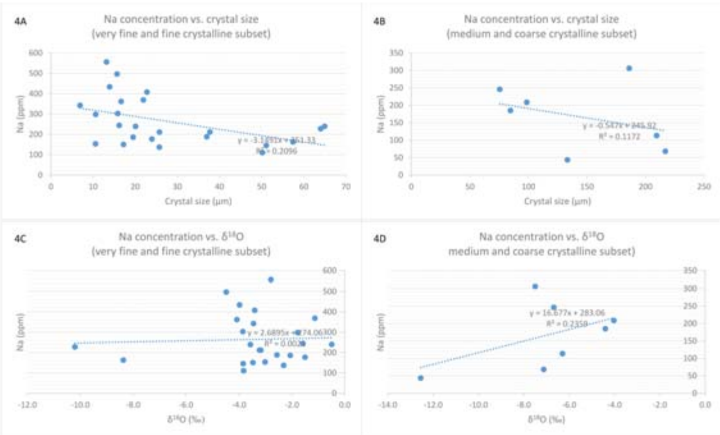

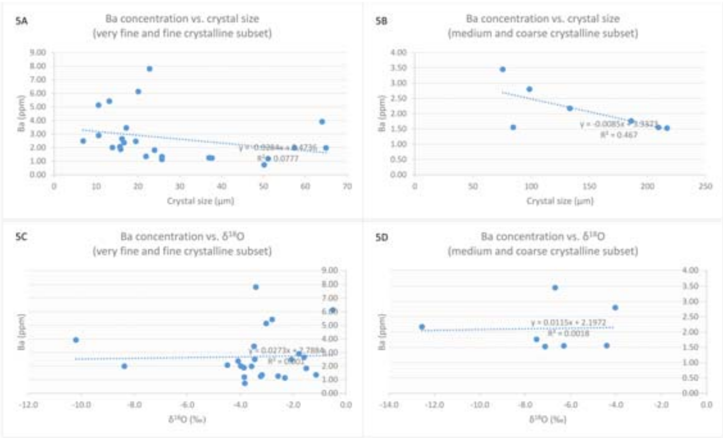
5A
Ba concentration vs. crystal size
(very fine and fine crystalline subset)
Ba (ppm)
Crystal size (µm)
5B
Ba concentration vs. crystal size
(medium and coarse crystalline subset)
Ba (ppm)
Crystal size (µm)
R² = 0.467
5C
Ba concentration vs. δ¹⁸O
(very fine and fine crystalline subset)
Ba (ppm)
δ¹⁸O (‰)
5D
Ba concentration vs. δ¹⁸O
(medium and coarse crystalline subset)
Ba (ppm)
y = 0.0115x + 2.1972
R² = 0.0018
δ¹⁸O (‰)

Origin of 'seismites' in Southern Tenerife
IAS Grant 2014 report

Helen Lacey, PhD student

Supervisors: Veerle Vandeginste, John Cosgrove (Imperial College London)

Introduction

Seismites, illustrations of seismic shocks in sedimentary rocks, provide evidence of historical seismic activity which may not otherwise be apparent (Montenat et al. 2007). These structures can help to work out the magnitude of the earthquake and distance to the epicentre (Allen 1986). They also indicate that during sedimentation a specific interval has been affected by seismic activity (Van Loon 2014). This can help reconstruct the tectonics of the area. Although classifications of these structures have been proposed (e.g. Montenat et al. (2007)), misinterpretation of them is common and can lead to incorrect conclusions being drawn about the geological history of a region.

Free standing elongated, cylindrical and tubular sandstone structures cemented by carbonate lie in the shadow of Montaña Bocinegro and Montaña Roja near El Médano, Tenerife. The current publicly communicated interpretation of these features is that they are products of liquefaction caused by a paleoearthquake ('seismites'), where water and sand were transported to the surface by ejection during hydraulic fracturing (González de Vallejo et al. 2005). Conversely, Kröchert et al. (2008) has interpreted those structures to have a biogenic origin using the general criteria diagnostic for rhizocretions and root tubules with respect to their orientation, size, branching system, and style of cementation. An interpretation of seismites would have implications for the seismic history and future of Tenerife, whereas rhizocretions would have implications for the historical climatic conditions on the island. Neither study has employed methods other than mapping, field analysis, microscopy and sample dating.

Methods

For this study, an interdisciplinary approach of fieldwork, microscopy (conventional and cathodoluminescence (CL)) and stable carbon and oxygen isotope analyses is employed to understand the formation of these sedimentary structures. The mineralogical and textural characteristics of the features (including chemical zonation of cement phases) and the outcrops surrounding the site are studied through mapping, sedimentological logging and microscopy. In addition, stable carbon and oxygen isotope analysis on the carbonate cements that lithified the sediment in the features determines a geochemical signature which provides information on the fluid source and interactions with the surrounding rock (Morad et al. 1990). Ratios are reported in per mill relative to Vienna Pee Dee Belemnite (VPDB) standard, by assigning a $\delta^{13}C$ value of +1.95‰ and a $\delta^{18}O$ value of -2.20‰ to NBS19 (Friedman et al. 1982).

Results

Fieldwork

The sedimentary features are pillar shaped sandstone structures composed of elongated, cylindrical concretions and joints cemented by carbonate with some infilled carbonate tubes and calcrete, randomly distributed across the site (Figure 1). They do not appear to be illustrative of liquefaction features; the soft deformation features described by Montenat et al. (2007) are much more like flow features as opposed to trunk like features and tubes.

Figure 1. Sandstone pillar features

At the south-eastern corner of the area where the majority of the sedimentary features occur, there is an outcrop capturing the stratigraphy of the area (Figure 2). González de Vallejo et al. (2005) identified this exposure as a fault; however, no displacement of stratigraphic sequences has been observed along this contact. Furthermore, there is no evidence of a water saturated sediment and an impermeable layer in the sandstone overlying the paleosol which would be required to permit upshoots of water to create the structures (Figure 2).

Figure 2. Stratigraphic exposure

Microscopy

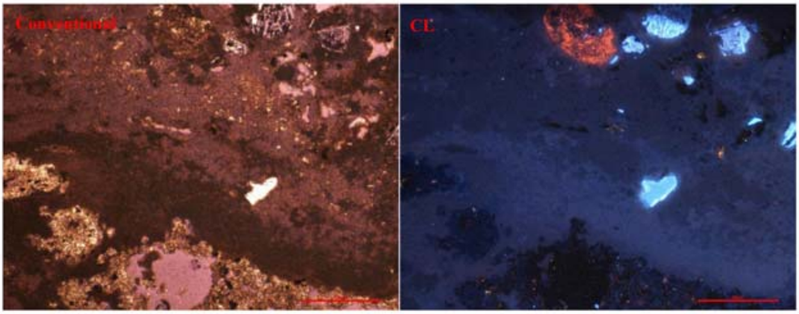

Figure 3. Microscopic images of cement fabrics within the sandstone tubes

Brown 'mottle' fabrics are clear in the conventional image and there are at least two distinct phases/generations of cement, clear in the CL image (Figure 3). Such fabrics are not typical of seismic/volcanic events. There is no evidence of any crystals changing their size, shape or orientation which would occur if the rocks were subjected to heat or stress (Jaroslow et al. 1996). Several cement phases are generally associated with slow precipitation from meteoric waters (Tucker 2009). The cloudy brown, micritic fabrics can be interpreted as organic material which are commonly associated with rhizocretions and calcrete (Horbury and Qing 2004).

Stable isotopes

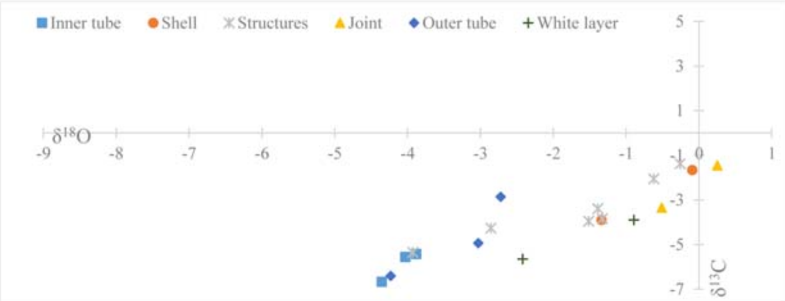

Figure 4. Stable isotope results of the carbonate within the tubes ('Inner tube'), the carbonate cement in the outsides of the tube features ('Outer tubes'), the cement in the jointing features ('Joint'), cements holding together the characteristic larger sandstone features, ('Structures'), shells found embedded in the paleosoil underlying the structures ('Shell') and the white calcrete ('White layer')

The $\delta^{18}O$ values in the cements range from -4.4 to -0.3‰ VPDB. The $\delta^{13}C$ values range from -6.4 to -1.4‰. If these structures were related to volcanic or seismic activity, they would show a much more depleted oxygen signature given the very high temperatures associated with these events, and a much tighter scatter if the structures were produced over a very tight time range. The strongly depleted carbon isotope values in the cements are inconsistent with a predominantly inorganic carbon source at depth (expected for volcanic or seismic activity, with fluids brought up from depth). However, such values are typical for meteoric fluids. Rhizocretions would explain the depleted isotopic signature of the cements within the tubes, as they uptake predominantly meteoric waters. The cements in the sandstone surrounding the tubes would have some input from seawater, closer to a 0‰ signature, hence the less depleted isotopic values i.e. there are two sources of fluids. The $\delta^{13}C$ of the shells found in the paleosol are close to what is expected for a marine signature; it is suggested that these could be a main source of carbon.

Conclusions

It is concluded that the studied structures are 'carbonate megarhizoliths' (Alonso-Zarza et al. 2008), evidence of root systems produced through the cycle of chemical weathering, decomposition, reprecipitation and cementation. Since the multiple interpretations of elevated seismicity in Tenerife in 2004, this conclusive study has importance for assessing seismic recurrence intervals in Tenerife, and for the characterisation of such structures.

References

Allen, J. R. L. (1986). "Earthquake magnitude-frequency, epicentral distance, and soft-sediment deformation in sedimentary basins." *Sedimentary Geology*, **46**(1), 67-75.
Alonso-Zarza, A. M., J. Genise, M. Cabrera, J. Mangas, A. Martín-Pérez, A. Valdeolmillos and M. Dorado-Valiño (2008). "Megarhizoliths in Pleistocene aeolian deposits from Gran Canaria (Spain): ichnological and palaeoenvironmental significance." *Palaeogeography, Palaeoclimatology, Palaeoecology,* **265**(1): 39-51.
Friedman, I., J. O'Neil and G. Cebula (1982). "Two New Carbonate Stable-Isotope Standards." *Geostandards Newsletter,* **6**(1): 11-12.
González de Vallejo, L. I., M. Tsigé and L. Cabrera (2005). "Paleoliquefaction features on Tenerife (Canary Islands) in Holocene sand deposits." *Engineering geology*, **76**(3): 179-190.
Horbury, A. D. and H. Qing (2004). "'Pseudobreccias' revealed as calcrete mottling and bioturbation in the Late Dinantian of the southern Lake District, UK." *Sedimentology,* **51**(1): 19-38.
Jaroslow, G. E., Hirth, G., & Dick, H. J. B. (1996). "Abyssal peridotite mylonites: implications for grain-size sensitive flow and strain localization in the oceanic lithosphere." *Tectonophysics*, **256**(1), 17-37.
Kröchert, J., E. Buchner and L. I. G. de Vallejo (2008). "Conspicuous sediment structures in fossil beach deposits (southern Tenerife, Canary Islands, Spain): paleoliquefaction features versus biogenic origin." *Marine Geophysical Researches*, **29**(3): 177-184.
Montenat, C., P. Barrier and C. Hibsch (2007). "Seismites: An attempt at critical analysis and classification." *Sedimentary Geology,* **196**(1): 5-30.
Morad, S., Al-Aasm, I. S., Ramseyer, K., Marfil, R., & Aldahan, A. A. (1990). "Diagenesis of carbonate cements in Permo-Triassic sandstones from the Iberian Range, Spain: evidence from chemical composition and stable isotopes." *Sedimentary Geology*, **67**(3), 281-295.
Tucker, M. E. (2009). "Sedimentary petrology: an introduction to the origin of sedimentary rocks." John Wiley & Sons.
Van Loon, A. J. (2014). "The life cycle of seismite research." *Geologos,* **20**: 61-66.

IAS Grant
Year-End Report

4/30/15

How do hiatal type and nutrient enrichment affect marine macrofossil abundance and preservation?

A case study in the Permian Phosphoria and Park City Formations

Preliminary Report to IAS

Since my 2014 field season was my first exposure to these rocks of the Phosphoria and Park City Formation, and involved a great deal of reconnaissance in poorly mapped areas, further field observations and data collection are necessary for me to confidently evaluate my hypotheses. Following my 2015 field season, I will send an additional report to IAS to more clearly detail my findings. I am investigating the parasequence-scale stratigraphic anatomy of several spatially distinct localities, as well as examining bioclast close packing, shell bed type, and taphonomy (biostratinomy and diagenesis) as a function of proximity to upwelling cells, physical energy, and hiatal type and duration.

The very base of the Meade Peak Member is known in all the mines as the "fish scale marker bed," and it is a thin, densely packed, silicified bed with phosphatized orbiculoid brachiopod and fish debris, generally considered to be superjacent to the first sequence boundary. This sequence boundary at the top of the Grandeur carbonates is marked by a smooth, undulatory paleo-karst surface with a 1-cm thick reddish-purple calcrete horizon. The Grandeur below has dispersed to loosely packed silicified shells; simple to complex shell beds are also present in some localities. The organic carbon- and phosphate-rich mudstones and shales of the Meade Peak Member often have dispersed to loosely packed fossils of inarticulate and articulate brachiopods, gastropods, ammonites, and some fish material preserved with calcite (secondary), phosphatized surfaces, or as molds. Shell beds are present primarily as stringers and pavements of calcite shell fragments within homogenous mudstones with calcareous cement. In contrast, the fine orange sandstone beds within the upper few meters of the Meade Peak Member, leading up to the maximum flooding surface, tend to yield dispersed moldic fossils of articulate brachiopods and gastropods, as well as manganese nodules. Within the Meade Peak Member, there is some parasequence-scale cyclicity, demonstrated by repetition of several distinctive lithologies; it is not yet clear where the beds of economic phosphorite fall within these cycles.

Particular horizons within the "center waste shale" of the Meade Peak Member are also characterized by laterally extensive (tens to hundreds of meters) concretionary horizons, as well as some discontinuous concretionary oblate spheroids. Depending on east-west position of the section, centimeter-scale ammonites, articulate brachiopods, or scaphopods may be affixed to the upper surfaces of these calcareous concretions, demonstrating a clear spatial gradient in faunal preservation in these beds.

IAS Grant 4/30/15
Year-End Report

The Rex Chert has at least three distinct lithologies, recognized in several localities. First, there are decimeter-scale beds of bluish-black massive chert with nodular surfaces; mm-scale ghosts of silicified skeletal material are dispersed to loosely packed throughout, and in some cases, fragmented or flattened brachiopod shells cover bedding planes. Second, gray to reddish silicified packstones, wackestones, and grainstones occur as part of the Rex, usually in the upper part of the unit. Third, some sections yield only translucent gray chert, with minimal evidence of bedding or fossiliferous content. When I receive my prepared thin sections to assess, I will have a clearer picture of how these unique units varied paleoenvironmentally, as sponge spicules were the silica source, but via different paths of diagenesis.

The younger Franson carbonates occur as continuous beds with distinctive parasequences, or as very fossiliferous lentils (also described as carbonate bioherms). These beds have a range of fossil content, containing densely packed beds of brachiopods or cm-scale crinoid ossicles, as well as dispersed debris of fish, brachiopods, bivalves, bryozoans, and crinoids; fossil material tends to be silicified or coarsely recrystallized calcite. Evidence of likely storm beds is present in one section, and this will certainly be a pathway of further investigation this field season. The Park City Fm carbonates do seem to have greater fossil content in beds sub- and superjacent to the Phosphoria Fm cherts and phosphatic members, possibly reflecting the beginnings or tail ends of enhanced nutrient enrichment.

During my 2014 field season I made many observations of features that require revisiting and further investigation to fully assess. Thus, this summer I will be focusing more on several specific parts of my questions to address the many vicissitudes of this record: for example, if deposits are storm-generated versus primarily the result of changes in relative sea level; variation in the characteristics of stratigraphically significant surfaces (SB, MFS, MRS) with respect to bioclast accumulations; and how the Bioturbation Index varies through the sections, as it relates to paleo-oxygenation. Much of my stratigraphic inquiry will be to test my null predictions for bioclast and bed properties in a sequence stratigraphic context, and then to determine whether or how any deviations are the result of paleo-upwelling conditions.

STRATIGRAPHIC HETEROGENEITY INDUCED BY ALLOGENIC AND AUTOGENIC FACTORS IN A PALEOGENE LOW NET-TO-GROSS FLUVIAL SUCCESSION, ARÉN-ESPLUGAFREDA, SOUTHERN PYRENEES, SPAIN

Oscar J. Arévalo

Fluvial & Eolian Research Group, School of Earth and Environment, University of Leeds, UK.

E-mail: eeoja@leeds.ac.uk

INTRODUCTION

The preserved sedimentary record of most fluvial successions is influenced by the interaction of one or more principal allogenic factors: tectonics, climate and eustasy (Catuneanu, 2006; Miall, 2013 and references therein). These factors are interdependent and their effects, in many cases, can be superimposed; consequently, discriminating their relative roles is not straightforward. For recent deposits, implementation of different radiometric, isotopic and palaeontological tools to constrain climatic, sea-level and tectonic changes often facilitates evaluation of the relative roles of allogenic factors. However, in ancient deposits, where the accessible information is more limited, this task is more complex. Additionally, the geometry of channel bodies and the evolution of surrounding floodplain elements in fluvial environments are also controlled by intrinsic (autogenic) factors such as bank erodibility and stream power and the preserved sedimentary signatures of such processes can mask allogenic controls.

The approach undertaken for this study has involved the acquisition of quantitative and qualitative sedimentological data from synorogenic Paleogene fluvial deposits of the Tremp-Graus basin, in the Arén-Esplugafreda sector, located in the central southern Pyrenees (Spain). The study of these deposits, informally known as 'upper red Garumnian' (Rosell et al., 2001), represents an ideal opportunity to evaluate the role of tectonics, climate and eustasy in controlling preserved fluvial architecture. Excellent time constraints exist for both the syn-sedimentary tectonic activity and the occurrence of climatic changes. Additionally, the regional and temporal context of the basin serves to constrain the extent and timing of eustatic influence. This knowledge of the nature of extrinsic controls on sedimentation has facilitated the interpretation of signatures present in the preserved lithological record of an ancient fluvial system in relation to these precursor allogenic drivers. Overall, this succession has been interpreted previously as the product of an ephemeral fluvial system in an arid environment (Dreyer, 1993), where multiple streams undertook repeated and apparently frequent avulsions. Therefore it is also possible to interpret the evolution of this fluvial system in terms of the intrinsic processes responsible of these multiple avulsions.

The main aim of this study is to document the heterogeneity of a low net-to-gross fluvial succession by means of acquisition of quantitative and qualitative sedimentological data, and to explain these lateral and vertical changes in terms of well constrained allogenic drivers. A secondary aim is to interpret particular conditions and controls on evolution of the depositional environment (autogenic factors). Specific research objectives are as follows:

- Acquisition of quantitative and qualitative sedimentological data from well-exposed outcrops of the Paleogene fluvial succession in the Arén-Esplugafreda sector;
- Interpretation of sedimentary processes and depositional subenvironments based on lithofacies and architectural elements defined;
- Comparison of results with existing data from other low net-to-gross fluvial successions worldwide in order to establish predictable relationships for different geological scenarios.

REGIONAL GEOLOGY

The study region covers an area of approximately 3 km^2 in the northern sector of the Tremp-Graus basin, a structural depression oriented in WNW-ESE direction and located in the central part of the South Pyrenean foreland basin, in north-eastern Spain (Figure 1). The 'upper red Garumnian' is laterally interbedded with marine calcareous deposits assigned to the Early and Late Tanethian (Pujalte et al., 2014). Analyses from different localities indicate the occurrence in the upper part of this unit of a negative carbon isotopic excursion (CIE) corresponding to the Paleocene-Eocene Thermal Maximum (PETM) (Manners et al., 2013; Dawson et al., 2014; Pujalte et al., 2014). The studied unit is overlain by a succession of marine limestone beds informally known as 'Alveolina Limestones' and assigned to the Paleocene-Eocene transition (Serra-Kiel et al., 1994). The 'upper red Garumnian' in the study area can therefore be assigned to the Late Paleocene (Thanetian) – Early Eocene.

The 'upper red Garumnian' is mainly composed of fine-grained red-coloured mudrocks that are massive or banded due to pedogenic processes, and which contain minor and apparently randomly distributed interbeds of sandy and gravelly channelized to poorly channelized bodies. In the uppermost part of this low net-to-gross succession, a conglomeratic interval occurs, which locally attains more than 10 m of thickness and which according to Schmitz and Pujalte (2007) extends for at least 500 km^2.

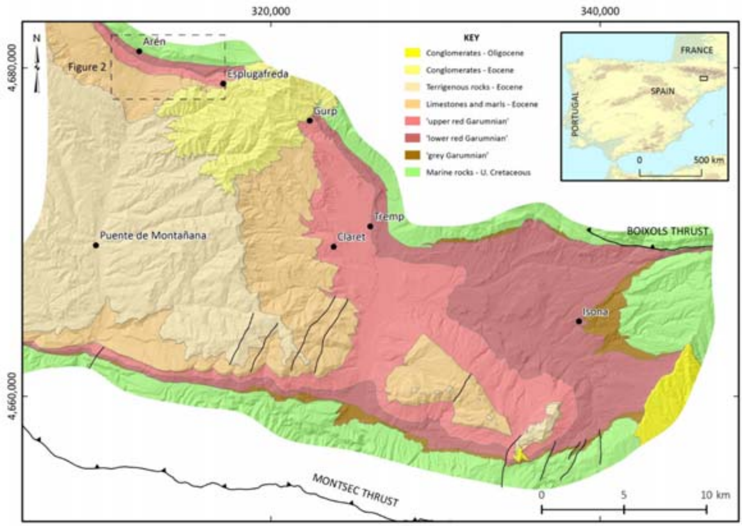

Figure 1. Regional geological map of the eastern sector of the Tremp-Graus basin.

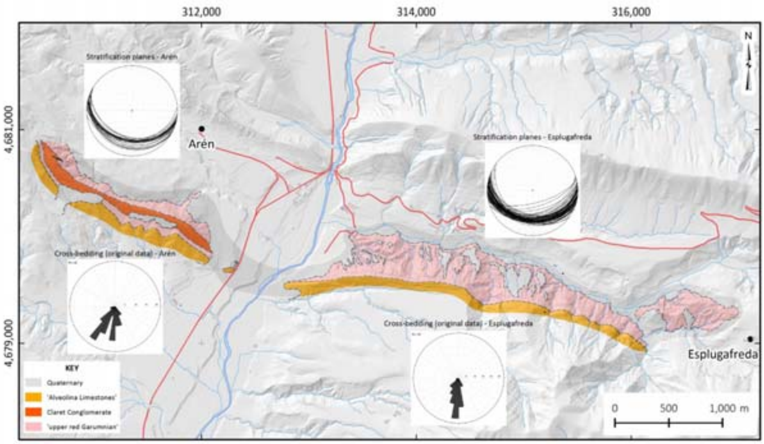

Figure 2. Local geological map of the Arén–Esplugafreda sector.

3

This body, named Claret Conglomerate by Pujalte and Schmitz (2005), is considered by different authors to represent a depositional event associated with the PETM (Schmitz and Pujalte, 2007; Pujalte et al., 2014, Manners et al., 2013; Dawson et al., 2014).

LOCAL GEOLOGY

Outcrops in the study area extend for over 6 km in WNW-ESE direction and are located in the vicinity of the town of Arén and the village of Esplugafreda (Figure 2). The exposures of the 'upper red Garumnian' are located in the southern slopes of the Esplugafreda Creek and an unnamed creek in the Arén sector. The 'Alveolina Limestones' overlay in apparent concordance the topmost fine-grained mudrocks of the 'upper red Garumnian'. In the Arén sector, the Claret Conglomerate occurs as a continuous body exposed for about 1.8 km, which locally attains about 10 m of thickness, and that can be mapped as a separated unit within the 'upper red Garumnian' (Figure 2). In the Esplugafreda sector, the thickness of the Claret Conglomerate is usually less than 4 m and it does not constitute a laterally continuous body; for this reason it has not been differentiated from the 'upper red Garumnian' for the purposes of this study.

Data relating to tectonic dip and strike of the bedding for the Arén section (n= 27) show dip direction values to the SSW. For the Esplugafreda section (n= 79) the data show a slightly increased dispersion, but still the dominant dip direction is SSW. The inclination angles of primary bedding surfaces range between 30° and 40°. The uniformity of these tectonic tilt data reflects the absence of folding in the studied sections. Dip-azimuth data relating to primary bedding and cross-bedding were plotted using the Stereonet software obtained from the Richard Allmendinger website and whose algorithms are described in Cardozo and Allmendinger (2013). For both sectors, the original cross-bedding data show a consistent dip orientation to the S and SSW (Figure 2).

RESULTS

Outcropping channel bodies have been mapped using high-resolution orthophotographs, LiDAR DEM's and GPS data; lithofacies associations and architectural elements have been characterized by field analysis. Two main facies associations of fluvial deposits are defined, which correspond to channelized bodies and overbank deposits. The channelized facies association comprises gravelly and sandy deposits arranged in four types of architectural elements, defined according to their geometry and internal architecture. Ribbon and poorly channelized sheet-like bodies represent single-storey channel-fill elements, whereas compound bodies and amalgamated complexes are formed by superposed channel-fill events under the prevailing conditions of low subsidence. According to the data collected so far, the different channelized elements identified are mainly composed of sandstones and conglomerates with horizontal lamination. Predominance of this kind of structures, indicative of transcritical to supercritical flow, have been associated with deposits from flash floods in ephemeral fluvial systems (cf. North and Taylor, 1996). The overbank facies association comprises extensive intervals of pedogenic altered floodplain siltstone, along with non-confined sheet-like bodies composed of bioturbated and pedoturbated very-fine-grained sandstone.

Although the 'upper red Garumnian' was deposited contemporarily with the initial phase of uplifting of the Pyrenees, it coincides with an interval of relative tectonic quiescence, as demonstrated by the absence of significant angular variations in the inclination of primary stratification through this succession. In consequence, the dominant allogenic drivers which controlled sedimentation were climate and eustasy. The existence of a hiatus in sedimentation, which coincides with the Chron C25n, could be associated with a eustatic change, however its imprint in the stratigraphic record of the studied area has not been identified with confidence.

The main changes in the lithological record observed in the 'upper red Garumnian' in the study area are associated with climatic factors and specifically with a precipitation increment in relation to the PETM. This precipitation increase would be responsible for the change in palaeohydrological conditions observed in overbank deposits from well-drained in the pre-PETM deposits to moderate to poorly-drained in the syn-PETM sediments. Additionally, this scenario of increased precipitations can be associated with a change in the power of streams, recorded in the predominance of massive conglomerates in the Claret Conglomerate, and a related increment in the bank erodibility, which favoured the lateral migration of channel-fill bodies.

FORTHCOMING PLANNED WORK

A third field season in the Arén–Esplugafreda sector of about 30 days is planned to be undertaken during April 2016 with the aim of acquiring data from all the channelized elements and measuring additional continuous stratigraphic sections in intervals mainly composed of overbank deposits. In this same field season, the acquisition of data from other areas with good exposures of the 'upper red Garumnian' (in the vicinities of Gurp and Talarn) will be undertaken in order to have other localities of reference for comparison. After the acquisition and compilation of a more complete dataset during this third field season, the preparation of a draft of a publication with the sedimentological interpretation of the 'upper red Garumnian' in the Arén-Esplugafreda sector and other localities of reference within the Tremp-Graus Basin will be undertaken.

IAS GRANT USE

The €1,000 IAS grant money was used for the partial payment of the accommodation expenses in Arén during a field season (September to October, 2015).

CITED REFERENCES

Cardozo, N., and R. W. Allmendinger, 2013, Spherical projections with OSXStereonet: Computers & Geosciences, v. 51, p. 193-205.

Catuneanu, O., 2006, Principles of Sequence Stratigraphy: Oxford, Elsevier Science, 386 p.

Dawson, A., S. Grimes, M. Ellis, R. Duller, M. Watkinson, M. Stokes, and M. J. Leng, 2014, Initial paleohydrological observations from the Paleocene-Eocene boundary at Esplugafreda and Berganuy in northern Spain: Rendiconti Online Della Società Geologica Italiana, v. 31, p. 54-55.

Dreyer, T., 1993, Quantified fluvial architecture in ephemeral stream deposits of the Esplugafreda Formation (Palaeocene), Tremp Graus Basin, northern Spain, *in* M. Marzo, and C. Puigdefábregas, eds., Alluvial Sedimentation, International Association of Sedimentologists, Special Publication No. 17, p. 337-362.

Manners, H. R., S. T. Grimes, P. A. Sutton, L. Domingo, M. J. Leng, R. J. Twitchett, M. B. Hart, T. D. Jones, R. D. Pancost, and R. Duller, 2013, Magnitude and profile of organic carbon isotope records from the Paleocene–Eocene Thermal Maximum: Evidence from northern Spain: Earth and Planetary Science Letters, v. 376, p. 220-230.

Miall, A. D., 2013, Fluvial Depositional Systems: Berlin, Springer International Publishing, 316 p.

North, C. P., and K. S. Taylor, 1996, Ephemeral-fluvial deposits: integrated outcrop and simulation studies reveal complexity: AAPG bulletin, v. 80, p. 811-830.

Pujalte, V., and B. Schmitz, 2005, Revisión de la estratigrafía del Grupo Tremp («Garumniense», Cuenca de Tremp-Graus, Pirineos meridionales). Geogaceta, v. 38, p. 79-82.

Pujalte, V., B. Schmitz, and J. I. Baceta, 2014, Sea-level changes across the Paleocene–Eocene interval in the Spanish Pyrenees, and their possible relationship with North Atlantic magmatism: Palaeogeography, Palaeoclimatology, Palaeoecology, v. 393, p. 45-60.

Rosell, J., R. Linares, and C. Llompart, 2001, El "Garumniense" prepirenaico: Revista de la Sociedad Geológica de España, v. 14, p. 47-56.

Schmitz, B., and V. Pujalte, 2007, Abrupt increase in seasonal extreme precipitation at the Paleocene-Eocene boundary: Geology, v. 35, p. 215-218.

Serra-Kiel, J., J. Canudo, J. Dinares, E. Molina, N. Ortiz, J. Pascual, J. Samsó, and J. Tosquella, 1994, Cronoestratigrafía de los sedimentos marinos del Terciario inferior de la Cuenca de Graus-Tremp (Zona Central Surpirenaica): Revista de la Sociedad Geológica de España, v. 7, p. 273-297.

Report for IAS Postgraduate Grant Scheme, 1st session of 2014

Qijian Li

GeoZentrum Nordbayern, University of Erlangen-Nürnberg, Germany

June, 2015

Title of the awarded project: Comparative analysis between the Late Ordovician mud-mound communities and non-reef communities in the Sanjushan Formation at Wu'ai, southeast China

Amount of money awarded: 990 €

Results:

(I) Laboratory work (fossil identification):

Previous studies shown that corals and stromatoporoids are common components in some reef-bearing strata of the upper Sanqushan Formation at the northern margin of the Zhe-Gan platform (Bian et al. 1996). However, polished slabs and thin sections of the our samples revealed that there were unreported massive macrofossils which were conspicuous, showing clusters of spheroidal to ellipsoidal chambers (Fig. 1A & D). Some of the chambers exhibit distinct exaulos (spout-like ostia), arising from mamelon-like protuberances. These fossils turned out to be *Corymbospongia* (sphinctozoans). In contrast to the silicified holotype from California (Rigby and Potter 1986), *Corymbospongia* at Wu'ai is embedded in massive limestone. Pervasive recrystallization of chambers displays no internal structures. Perforate walls and prominent exaulos are the two most valuable characters for identification. The irregular polygonal or rounded rectangular shape of chambers shown in some plane sections of *Corymbospongia* (e.g. Fig. 1D) can lead to confusion with massive corals, which often show a similar arrangement of "chambers" on weathered surface.

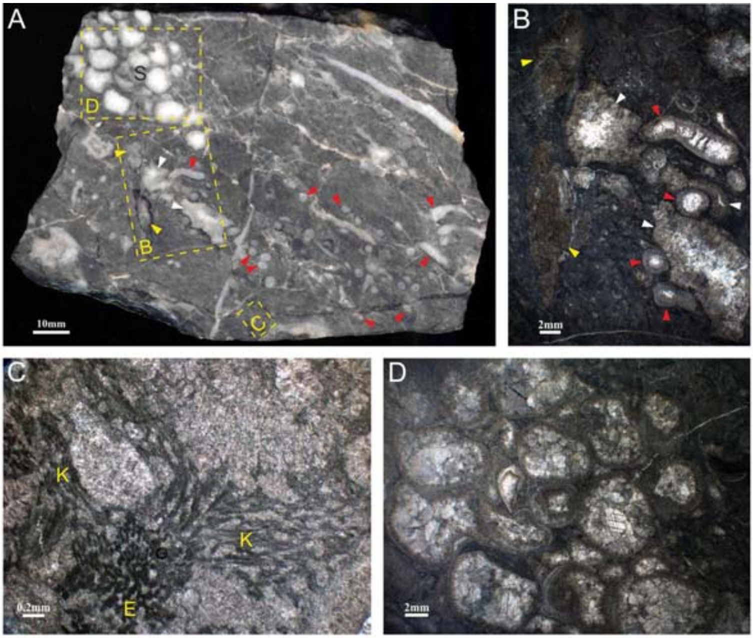

Figure 1 Biota and microfacies of the Wu'ai reef. A) Polished slab of sphinctozoan-coral-microbial boundstone. B-D) Thin-sections of rectangles marked in A. White triangles— cavities; yellow triangles—*Streptelasma*; red triangles—*Palaeophyllum*; S—sphinctozoan (*Corymbospongia*); E—*Epiphyton*; K—*Kordephyton*.

Bushy calcimicrobe is dominant in thrombolites of Wu'ai reef, showing a fan-like aggregation of bundled micritic filaments (Fig. 1C). Many of the filaments appear sinuous. These are 10-50 μm in diameter and have indistinct margins. Bian et al. (1996) erected a new genus (*Trichonophyton*) for the branching filamentous calcimicrobe, which is the major builder of the Huipu reefs (8 km southwest of Wu'ai). *Trichonophyton* was described as a bush-like thallus composed of numerously erect (or bent) branching filaments which are thinner and more slender than those of *Epiphyton*. Given that all described features of *Trichonophyton* agree with *Kordephyton* (Radugin & Stepanova 1964), we consider *Trichonophyton* a junior synonym of *Kordephyton* after discussing with the colleagues in the Nanjing Institute of Geology and Paleontology. Similar to Cambrian thrombolites (Elicki 1999; Kruse and Reitner 2014; Lee et al. 2014), *Kordephyton* also co-occurs with *Renalcis* and *Epiphyton* as important reef constructors in our case.

(II) Fieldwork:

There are two target sections (Zhuzhai section & Wu'ai section), representative of nearshore areas (shallow subtidal zone) and deeper subtidal environments of the Zhe-Gan platform (Fig. 2B).

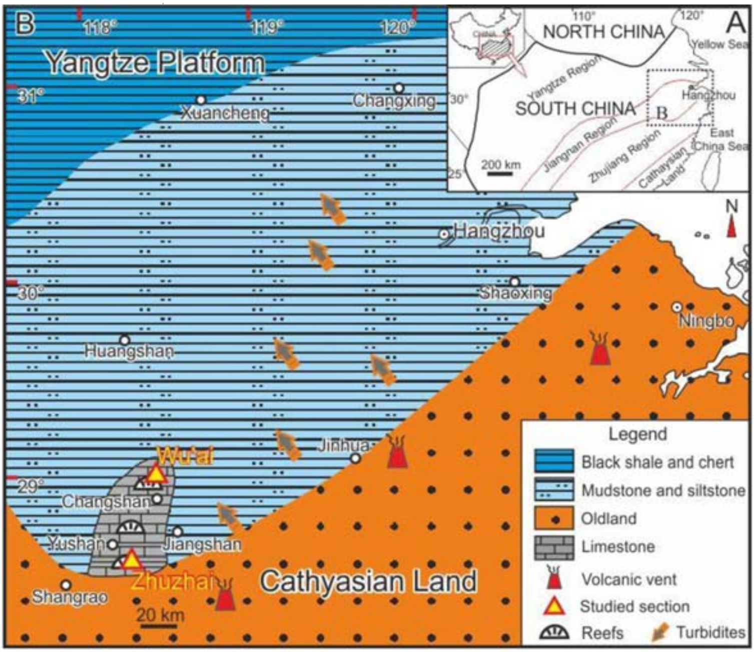

Figure 2 Location of the the sections (modified from Zhang et al., 2007). A) Depositional zones of South China in the Ordovician. B) Palaeogeography of the Jiangshan-Changshan-Yushan area, NW Zhejiang and S. Anhui during the late Katian (enlargement of the area indicated by dotted rectangle in A).

Zhuzhai section:

On the Zhe-Gan platform, the best-known example of coral–stromatoporoid reefs is exposed in the Xiazhen Formation at Zhuzhai (Yushan County, Jiangxi Province). The reefs occur in the lower part of the formation. They consist of stacked bioherms, which are 7.4m thick and over 20m wide. The reef complex contains two main reefal units. Below the first unit, there is a thick layer (around 1.1m) of brachiopod limestone that consists of a monospecific assemblage of large *Tcherskidium*, often in growth position. In 2013, we quantified the framework density and main constructional biota of the two reefal units by line transects. However, we did not get enough counting points (at least 100 points) for the second unit due to the limited time available in the field. And, we did not collect any data from the reef base (brachiopod limestone). In order to trace continuous changes of relative abundance of each component, point counting for macrofossils was carried out with line transects for the brachiopod limestone this time. Additional measurement on the second unit has been done at the same time. Based on the data collected in the outcrop, significant succession of fauna was confirmed in the reef from base to top.

Previous studies indicated that the Xiazhen Formation at Zhuzhai is continuous throughout the exposures from northwest to southeast with a thickness of more than 204 m. This view has been almost exclusively adopted by subsequent studies (e.g. Zhang et al. 2007). Recently, exposures of the Xiazhen Formation in the same locality were re-measured and described by a group of Korean geologists. The results revealed that the sub-sections in vicinity overlap stratigraphically. A thrust fault system appeared to be responsible for the repetition in the subsections (Lee et al. 2012). In 2013, we first recognized a paleokarst surface on the top of the second reefal unit of one of the subsections, suggested by mud cracks and large-scale erosional features. We would expect that identical lithological succession and sedimentation characteristics can be trace in repetition horizons of the other subsection if the new explanation is right. In this field trip, we confirmed that a paleo-weathering crust (kaolinite-bearing mudstone) (Fig. 3) overlaying on coral rudstone in another subsection. The paleo-weathering crust was first reported by a Chinese literature (Chen et al. 1987), but it was ignored by subsequent studies. We agreed that the coral rudstone here represent a margin of the bioherm (Lee et al. 2012) that we carried out point counting. And the paleo-weathering crust can be treated as a counterpart of the paleokarst surface on the top of the bioherm. Combined with the palaeontological, lithological and stable carbon isotope data (Munnecke et al. 2011; Lee et al. 2012), we are inclined to the repetition explanation, which will be helpful to understand the faunal and environmental changes in this area.

Figure 3 Field aspects at Zhuzhai. A) Greenish grey to purple reddish mudstone overlaying on coral rudstone. B) A brachiopod found in the greenish grey mudstone.

Wu'ai section:

The studied site (29° 00'15"N, 118°32'17"E) is located next to Wu'ai village of Songfan Town, some 11 km to the north of Changshan. In the study area, the upper part of the Sanqushan Formation is characterized by dark grey micritic limestone, and muddy nodular, bioclastic limestones alternating with microbialites (Zhang et al. 2007). Based on the skeletal macrofauna (brachiopods, corals and stromatoporoids) and a regional correlation, the upper part of the Sanqushan Formation is synchronous with the nearshore Xiazhen Formation of late Katian age, probably corresponding to the *Dicellograptus complexus* biozone (Zhang et al. 2007). At Wu'ai, the Upper Sanqushan Formation is exposed in an active quarry, which is approximately 230 m wide and 40 m high (Fig. 4A). Massive microbial boundstone prevails. Traces of bedding suggest that the entire reef is tilted near vertically. The base of the section is covered; the top is conformably overlain by the Wenchang Formation, which is characterized by grey-green, thick-bedded to massive calcareous, fine-grained sandstone with silty mudstone.

Figure 4 Field aspects of the Wu'ai reef. A) Panoramic view of part of the outcrop in the quarry, showing massive reef limestones. Vehicle (rectangle) = 1.95m. B) Vertical surface of microbial boundstone with sphinctozoans (red triangles), a few cavities (yellow triangles) and fractures (white triangles). Hammer = 27cm. C) Close-up of the boundstone showing sphinctozoan colonies (*Corymbospongia*) with clusters of spheroidal to ellipsoidal chambers (red triangles). Yellow triangle is stromatactis.

The size of reef was measured by using a laser rangefinder. The thickness of exposed reef limestone is approximately 120 m. The reef is mainly composed of massive microbial boundstone with a low abundance of in situ metazoans, predominantly sphinctozoan sponges (*Corymbospongia*) and rugose corals (mostly *Palaeophyllum* and *Streptelasma*) (Figs. 4B, C). Point counting for macrofossils was carried out with line transects on the outcrop. Although *Corymbospongia* is locally common (up to 13%), the overall contribution of sponges and corals to the reef limestone is low (altogether <15% in the densest areas). Stromatactis cavities of around 1.6-2.3 cm diameter are common (about 6% on average).

References:

Bian LZ, Fang YT, Huang ZC (1996) On the types of Late Ordovician reefs and their characteristics in the neighbouring regions of Zhejiang and Jiangxi Provinces, South China. In: Fan JS (ed) The ancient organic reefs of China and their relations to oil and gas. Marine Press, Beijing, China, pp54-75 (in Chinses)

Chen X, Rong JY, Qiu JY, Han NR, Li LZ, Li SJ (1987) Late Ordovician stratigraphy, sedimentology and environment of Zhuzhai of Yushan, Jiangxi. Journal of Stratigraphy 11:23-34 (in Chinses with English abstract)

Elicki O (1999) Palaeoecological significance of calcimicrobial communities during ramp evolution: an example from the Lower Cambrian of Germany. Facies 41:27-39

Kruse PD, Reitner JR (2014) Northern Australian microbial-metazoan reefs after the mid-Cambrian mass extinction. Memoir of the Assosiation of Australasian Palaeontologist 45:124-138

Lee DC, Park J, Woo J, Kwon YK, Lee JG, Guan L, Sun N, Lee SB, Liang K, Liu L, Rhee CW, Choh SJ, Kim BS, Lee DJ (2012) Revised stratigraphy of the Xiazhen Formation (Upper Ordovician) at Zhuzhai, South China, based on palaeontological and lithological data. Alcheringa: An Australasian Journal of Palaeontology 36:387-404

Lee JH, Lee HS, Chen J, Woo J, Chough SK (2014) Calcified microbial reefs in Cambrian Series 2, North China Platform: Implications for the evolution of Cambrian calcified microbes. Palaeogeogr Palaeocl 403:30-42

Munnecke A, Zhang YD, Liu X, Cheng JF (2011) Stable carbon isotope stratigraphy in the Ordovician of South China. Palaeogeogr Palaeocl 307:17-43

Radugin KZ, Stepapanovava MV (1964) Onitchatykh vodoroslyakh dokembriya severo-zapadnoy chasti Vostochnovo Sayana. 60-64 in Materialy po geologii i poleznym iskopaemym Zapadnoy Sibiri. Tomskiy Gosudarstvenniy Universitet, Tomsk

Rigby JK, Potter AW (1986) Ordovician Sphinctozoan sponges from the Eastern Klamath Mountains, Northern California. Memoir of The Paleontological Society 20:1-47

Zhang Y, Chen X, Yu G, Dan G, Liu x (2007) Ordovician and Silurian rocks of northwest Zhejiang and northeast Jiangxi provinces, SE China. University of Science and Technology of China Press, Hefei

Publication:

A manuscript about the preliminary results of the Wu'ai reef mentioned above was finished and submitted to *Facies* in March. And it was just accepted at the end of May:

Li QJ, Li Y, Kiessling W (2015) The first sphinctozoan-bearing reef from an Ordovician back-arc basin. Facies Accepted. DOI: 10.1007/s10347-015-0444-6

Ongoing work:

With the quantitative data collected from the field, further comparison between the reef and the non-reef communities in the Sanjushan Formation is under way. The paleogeographic pattern of the reefs and its main controlling factors are worth to discuss in details. Furthermore, the potential relation between the Boda event and reef development on the Zhe-Gan platform will be studied based on the local cases and the data extracted from the PaleoReefs database (http://www.paleo-reefs.pal.uni-erlangen.de/). The second publication about this project is going to be finished in the second half of this year.

IAS PGS Grant 2014 – A.J. Vellinga

National Oceanography Centre, University of Southampton Waterfront Campus SO15 3ZH Southampton

RECONSTRUCTING THE FORMATION PROCESSES OF THE SUPERCRITICAL SEDIMENTARY STRUCTURES, FAVIGNANA (ITALY); A NUMERICAL APPROACH

Proposal (250 words)

A submarine carbonate ramp on the island of Favignana has been studied by Slootman et al., in prep. Within this carbonate ramp-platform system, distinct bedforms now interpreted to be cyclic steps have been observed. This study aims to numerically reconstruct the sedimentary structures as found within the Favignana Calcarenites in order to provide a quantification on the conditions at which the sediments, with their specific architecture and structure, have been deposited. This is not only relevant in testing the hypothesis that the sedimentary structures as observed on Favignana are created by Froude-supercritical flow, but also in a broader sense provides a quantification on which turbidity currents are responsible for similar sedimentary features in the geological record and on the modern seafloor.

Some initial simulations on a 2-D geomorphic surface provided by Slootman et al. in prep. yielded very promising initial results of synthetic sedimentary structures related to Froude-supercritical flow, hence numerically simulation of density flows creating such deposits is feasible. A visit to the field in Favignana would be useful in the acquisition high-quality data on geomorphic surfaces and sedimentary structures, as well as in describing the overall facies. The outcrops on the Island of Favignana are of unique quality, given they are exposed in an old quarry which allows for a three-dimensional picture on the sedimentary structures. Favignana might be one of the few locations on earth providing enough high-quality data. Which is required in creating a solid two-dimensional, or even three-dimensional numerical simulation as proposed herein.

How the money was spent

As the proposal states, a field trip to Favignana has been conducted. During this field trip Arnoud Slootman has been so kind to show me some of the geology of Favignana, and also the Favignana calcarenites of interest.

We have spent about five days in the field on Favignana. Firstly the regional geology of Favignana has been explored. Arnoud Slootman has spent quite a while on the Island so could bring me up to speed on the geology quickly. We have discussed the cool water carbonate system from shoreface to offshore deposits, focussing on to slope-ramp clinoforms to more distal toeset deposits. Secondly, we have spent most time looking at the outcrops at San Vituzzo. The outcrops in San Vituzzo are of such world-class that they can be used to constrain paleo-bathymetries and grain-properties, which are input parameters needed for forward modelling, as proposed in the proposal of grant application. These outcrops are also ideal to deduct the processes at play depositing the calcarenites as found, Arnoud and I have spent a lot of time discussing processes as well, and we feel we have come to a more detailed understanding. Lastly, we have visited two sites on mainland Sicily, of calcarinitic systems of similar age and setting, to compare their characteristics to those on Favignana.

The money was partly spent on flights to and from Sicily (LHR-PMO and PMO-VIE), accommodation near the field-location, transportation on the spot - both by car and bicycle – and food etc. The total expenses exceed the 1000 Euro grant amount, so the difference will have to be funded in another way.

What results have been obtained?

The Favignana calcarenites at San Vituzzo mainly comprises of coarse calciclastic material, two main types of beds are observed. (1) Clear dune-like beds ranging from 0 up to about 10m in thickness, and laterally very variable changing several metres in thickness over a distance of less than 100m. (2) Equally laterally variable are beds showing low-angle cross-laminations, scours and massive scour-fills, thought to have originated from Froude supercritical flow.

The obtained results are first of all a better understanding of Froude-supercritical deposits by me and Arnoud. Secondly, and more quantifiable is that I have been able to acquire input parameterization for the numerical model; paleobathymaties/geomorphic surfaces and grain properties of the sediment. Such input parametrization is crucial for forward modelling, hence this would not have been possible without the IAS grant scheme. The modelling itself can now be done, but will not be consuming significant amounts of funding. I hope to be able to present some results of this study the coming year – although Krakow will be too close. The third outcome is that Arnoud Slootman and I aim to cooperate towards a publication on the Favingnana modelling efforts, and Froude-supercritical density currents in general.

I would again like to thank the IAS for making this possible through the PGS grant scheme.

Kind Regards,

Age Vellinga

ANNOUNCEMENT

IAVCEI-IAS 6IMC

6TH INTERNATIONAL MAAR CONFERENCE

Maar and Environment Change

[1, *] JING WU, [2] KÁROLY NÉMETH

[1] INSTITUTE OF GEOLOGY AND GEOPHYSICS CHINESE ACADEMY OF SCIENCES (IGGCAS), Beijing, P. R. China
[2] MASSEY UNIVERSITY, INSTITUTE OF AGRICULTURE AND ENVIRONMENT, Palmerston North, New Zealand
* E- mail: wujing@mail.iggcas.ac.cn

Between 30st July and 3rd August, 2016, the 6th International Maar Conference will be held in Yifu Teaching Building, Nanling Campus, Jilin University, Nanguan District, Changchun City (43°51'50.46"N; 125°19'49.96"E), Northeast China (Fig. 1). The Conference will have 4 days of themed oral and poster sessions and an intra-meeting field trip. The proposed sessions of the conference focus on **Maar and Environment Change**, covering a wide spectrum of very interesting topics including 1) characteristics, mechanism, modeling and geological background of monogenetic volcanism; 2) the volcanic evolution and spatial distribution small-volume volcanoes forming volcanic fields, 3) sedimentary facies architectures of monogenetic voclanoes such as syn-eruptive pyroclastic sedimentation, erosion related processes and the sedimentary systems of maar lakes, 4) resources relevant to monogenetic volcanoes with special relevance to maar-diatreme volcanoes including kimberlite pipes, 5) volcano disasters associated with monogenetic volcanoes, and 6) the detecting, monitoring and societal responses of volcanic activity associated with monogenetic volcanoes with a special focus on maar-diatreme volcanoes. During the conference a strong focus will also be given on researches and advances in studies associated with understanding the geoheritage, geoconservation, geotorusitic and geoeducational values of monogenetic volcanoes.

Environmental change does not only include physical changes like climate change, but also geological processes such as natural disasters, human

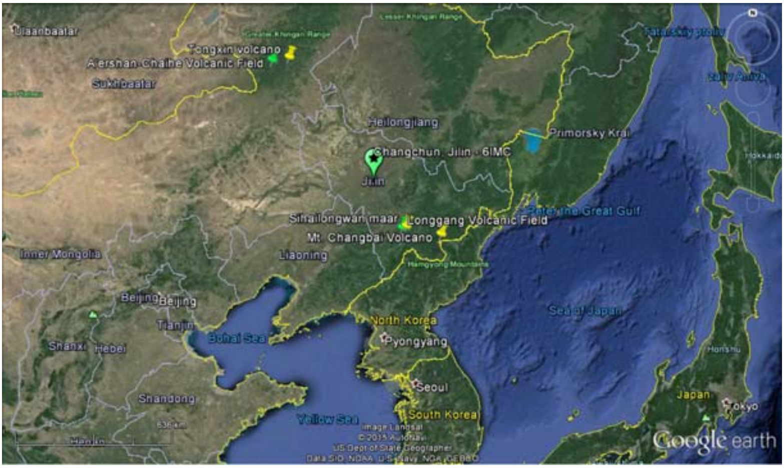

Figure 1.- Overview map of NE China and its surroundings with reference to the 6IMC conference site

interference, or animal interaction. The study of environmental change is growing fast as it related to the change or disturbance of the environment caused by human influences or natural ecological processes. For these kind of studies, the sediments of maar play an essential role in the reconstruction of environmental and climate change with an annual to decadal resolution.

Most of maar lakes are created by explosive eruptions through phreatomagmatic fragmentation of magma which occurs when rising magma interacts with groundwater. Depending on the depth of magma-water interaction, the explosion will cut the country rocks to make a deep or shallow crater, which could be either dry or water-filled depending on how water can access the newly formed crater from the disrupted groundwater table and how the crater can hold the water from normal rainfall. Once the maar lake formed, it will roughly go though four phases: 1) empty maar lake stage: *the maar is formed right now and has not yet collected water to form a crater lake*; 2) maar lake stage: *there are water and sediments in a maar lake*; 3) peat-bog-type maar lake stage: there is no water in the crater, it is filled up with terrestrisal sediments, however some wet grassland and swamp vegetation are in it; and 4) dry-out maar lake stage: *this type of maar lakes have dried out entirely and they just appear as a shallow negative landforms that is «carved» in to the earlier deposited lacustrine sediments*. During this evolution process, the signal of environmental change can be well preserved in the sediment of maar recording several millenia of terrestrial sedimentation that influenced under various climatic conditions

Maar lakes have indeed many advantages incomparison with other types of lake basins on forming and preserving high-resolution sediments (Fig. 2). The depth of maar lakes ranges from several meters to well over hundred meters. The lake depth to the lake surface area ratio of maars is larger than

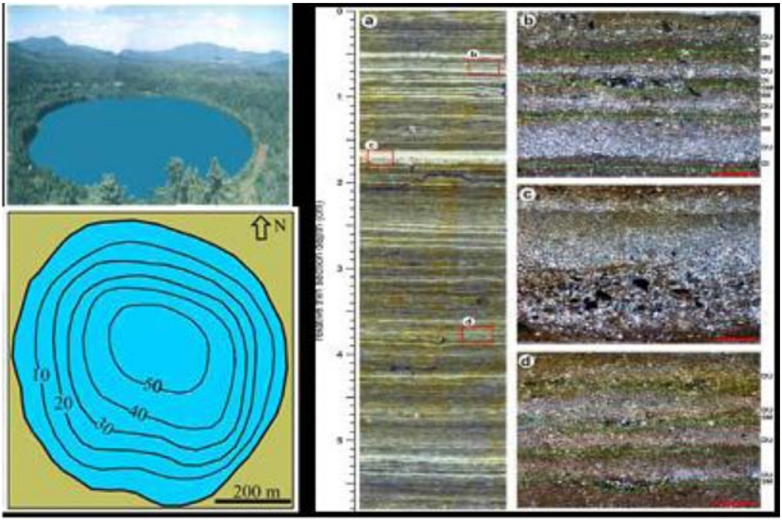

Figure 2.- Aerial photograph and bathymetric map (in metres) of Lake Sihailongwan (42°17'15.72"N; 126°36'7.65"E), Longgang Volcanic Field (mid-conference fieldtrip included in registration) and its Early Holocene micro-facies of varves from sediments of this lake.

other types of lakes. Therefore, maar lakes can provide anoxic condition, in which most of the large creatures and vegetation can not live letting the sediment accumulate slowly without bioturbation. The flat bottom of the maar lake also reduces the sedimentary disparity caused by the difference of topography/bathymetry of the lake floor. Both of the above conditions are to the benefit of the formation of the varves. As the dating beyond the range of radiocarbon is problematic, the age estimates for records over 50 ka rely on indirect dating approaches such as recognition of known tephra layers accumulated in the narrow sedimentary trap of a maar. The sediment sequences of maar lakes with varves therefore can provide great and diverse methods to apply and allow the establishment of varve-chronology, combined with calibration of ^{14}C up to 50 ka, tephrochronology and magnetostratigraphy to establish the accurate high resolution chronology for the reconstruction of paleoclimate and paleoenvironment.

Maar lakes are some small closed lakes with circular pyroclastic rims, whose catchment are similar with the lake surface's area resulting in that the water surface equilibrium is mainly controlled by the precipitation and the evaporation. The sedimentation rate and the chemical compositions also depend closely upon the hydrological system of the maar lakes. The hydrology and hydrogeology, the microorganisms, and internal parameters are mainly represented by the hydrothermal system beneath them. It implies that the multiproxies of sediment sequence in maar lakes like physico-chemical, biological, isotopic and geochemical compositional evolution can be used to

Figure 3.- Base surge dominated pyroclastic succession of Tongxin volcano (47°34'28.80"N; 121°17'31.02"E) from the A'ershan-Chaihe Volcanic Field (pre-conference field trip site).

reflect the effects of environment and climate change. The proxies of sediment records from maar lakes are much more abundant than that of any other high-resolution records like ice cores and stalagmites.

As a result of this increased research on using the sediment records from maar lakes to reconstruct paleoenvironment and paleoclimate, the **6th International Maar Conference** will place emphasis on to be a scientific conference for experts in any aspects of **Maar and Environment Change**.

The conference also will offer avenue to discuss pyroclastic processes and their influences to the total sedimentary budget a monogenetic volcanic field can provide to the terrestrial sedimentary record. Presentation of new methods, field studies, analogue and/or numerical modelling on pyroclast transport associated with lava fountains, scoria cones, tuff rings, maar-diatremes (Fig. 3) and small-volume lava dome formations will provide a good forum for the participants to understand these small-volume volcanoes from their volcanic origin to their useful nature to develop our view on the terrestrial sedimentary record.

Date:

Conference: 31st July (Sunday) – 3rd August (Wednesday) 2016

Icebreaker: 30th (Saturday) July 2016 evening

Intra-congress field trip to Longgang Volcanic Field (included in registration)(Fig. 1): 2nd (Tuesday) August 2016

Closing ceremony: 3rd (Wednesday) August 2016

Field trips

Pre-congress field trip takes place between 28th (Thursday) July – 30th (Saturday) July 2016 – 3 days (2 nights). Field trip to the A'ershan-Chaihe Volcanic Field (Fig. 1).

Post congress field trip takes place between 4th (Tuesday) - 6th (Saturday) August 2016 – 3 days (2 nights). Field trip to Mt. Changbai Volcano [42° 0'46.45"N; 128° 2'42.68"E] (Fig. 1)

Location/Venue

Changchun, China

Room 516, Yifu Teaching Building, Nanling Campus, Jilin University

Local Organising Committee

Chair of Conference:

Jiaqi Liu (Institute of Geology and Geophysics, Chinese Academy of Sciences)

Co-Chair:

Fengyue Sun (Jilin University)

Fuyuan Wu (Institute of Geology and Geophysics, Chinese Academy of Sciences)

Karoly Nemeth (Massey University)

Zhoubo, Changbai (Mountain Protection and Development Zone of Jilin Province)

Members:

Jule Xiao (Institute of Geology and Geophysics, Chinese Academy of Sciences)

Qiang Liu (Institute of Geology and Geophysics, Chinese Academy of Sciences)

Wenliang Xu (Jilin University)

Yongwei Zhao (Institute of Geology, China Earthquake Administration)

Zhengfu Guo (Institute of Geology and Geophysics, Chinese Academy of Sciences)

Zhongxia Zhou (Institute of Geology and Geophysics, Chinese Academy of Sciences)

Abstract Submission

1st January – 1st July 2016

Notification of Acceptance of Abstracts

1st July 2016

Abstract Format

2 page extended abstract format (template will be available on the web site)

Registration

1st January - 15th July 2016

Website

http://imc.csp.escience.cn/

Scientific Support

IAS

IAVCEI

IAVCEI Commission on Monogenetic Volcanism

IAVCEI Commission on Volcanic Lakes

IAVCEI Commission on Volcanogenic Sediments

IAVCEI Commission on Volcanic Geoheritage and Protected Volcanic Landscapes

Frames of the World

Polish Carpathian Foredeep

Sand pit near Suskrajowice. Upper shoreface sandstones of spit-bar platform (alternation of trough cross-stratification and inclined (10–20°) planar parallel stratification). More details on geology are in LeszczyD´ski, S. & Nemec, W., 2015. Sedimentation on the Serravalian forebulge shelf of the Polish Carpathian Foredeep. In: Haczewski, G. (ed.), Guidebook for field trips accompanying IAS 31st Meeting of Sedimentology held in Kraków on 22nd–25th of June 2015. Kraków, pp. 5–23. Guidebook is available online at www.ing.uj.edu.pl/ims2015 Polskie Towarzystwo Geologiczne 2015, ISBN 978-83-942304-0-1 (Photo by V. Pascucci)

INSTITUTIONAL IAS GRANT SCHEME (IIGS)

IIGS Guidelines

Special IAS Grants or Institutional IAS Grants are meant for capacity building in third world countries. There exists a list of 'Least Developed Countries' (LDC) by the UN. This list categorizes countries according to income per capita and is yearly updated.

Grants are allocated to allow Geology Departments in LDC to acquire durable sedimentological equipment for teaching and research (like sieves, calcimeters, auger drilling tools, etc.) or tools that can be used by all geology students (like general geology/sedimentology textbooks, IAS Special Publications (SP), memory sticks with back issues of Sedimentology or SP, etc). Therefore, the grant application should clearly demonstrate to increase the recipient's capacity to teach sedimentology at the undergraduate level (Bachelor) in a durable way. It should also indicate in what way it would enable to support sedimentological research at the graduate level (Master).

Applicants should have a permanent position at their University and should be IAS Full Members. Applications should be submitted by email to the Office of the Treasurer (ias-office@ugent.be) and contain the following information (not exhaustive list):

- the mission statement of the University/Geology Department
- the approval of the University Authorities to accept the grant
- a list of permanent teaching and technical staff members of the Geology Department (with indication of their area of research)
- the structure of the geology undergraduate and graduate courses (Bachelor/Master programme with indication of courses and theoretical and practical lecture hours)
- the number of geology students
- the actual facilities for geology/sedimentology students
- a motivation of application
- a budget with justification
- the CV of the applicant, including a sedimentology research plan

The institutional grant scheme consists each year of 2 sessions of 1 grant of 10.000 Euro. Applications run in parallel with the PhD research grant scheme (same deadline for application and recipient notification). The IAS Grant Committee will seek recommendations from relevant National Correspondents and Council Members (eventually including visitation) before advising the IAS Bureau for final decision. Additional funds made available by the recipient's University are considered as a plus.

Items listed in the application will be bought through the Office of the IAS Treasurer and shipped to the successful applicant. By no means money will be transferred to the grant recipient.

POSTGRADUATE GRANT SCHEME (PGS)

PG Guidelines

IAS has established a grant scheme designed to help PhD students with their studies by offering financial support for fieldwork, data acquisition and analysis, visits to other institutes to use specialized facilities, or participation in field excursions directly related to the PhD research subject.

Up to 10 grants, each of about 1,000 Euro are awarded, twice a year. These grants are available for IAS Student Members only. Students enrolled in MSc programs are not eligible for funding and research grants are not given for travel to attend a scientific conference, nor for the acquisition of equipment.

Applicants should apply for a postgraduate grant via the IAS website. The application requires submitting a research proposal with budget and CV (template provided on the submission webpage) and a letter of support from the student's supervisor. After the deadline has passed, the IAS Bureau evaluates the submitted applications and makes a final selection. Applicants are personally informed by the Office of the Treasurer about their grant. The grants are transferred to the applicants' bank account upon submission of a short scientific and financial report.

Eligibility and selection criteria:

- Applicants must be enrolled as a PhD student;
- Applicants can only benefit from a postgraduate grant once during their PhD;
- In the evaluation process preference will be given to those applications that i) can convincingly demonstrate that the proposed work cannot be conducted without the grant, and ii) are not supported by substantial industry funding.

Application

The application should be concise and informative, and contains the following information (limit your application to 1250 words max.):

- Research proposal (including Introduction, Proposal, Motivation and Methods, Facilities) – max. 750 words
- Bibliography – max. 125 words
- Budget – max. 125 words
- Curriculum Vitae – max. 250 words

Your research proposal must be submitted via the Postgraduate Grant Scheme application form on the IAS website before the application deadline. The form contains additional assistance details for completing the request. Please read carefully all instructions before completing and submitting your application. Prepare your application in 'Word' and use 'Word count' before pasting your application in the appropriate fields.

A recommendation letter from the PhD supervisor supporting the applicant is mandatory, as well as a recommendation letter from the Head of Department/ Laboratory of guest institution in case of laboratory visit. The letter needs to be uploaded by the candidate, when submitting his/her application, and not be sent separately to the Office of the Treasurer.

Please make sure to adequately answer all questions.

Deadlines and notifications

Application deadline 1st session: 31 March.

Application deadline 2nd session: 30 September.

Recipient notification 1st session: before 30 June.

Recipient notification 2nd session: before 31 December.

NOTE: Students who got a grant in a past session need to wait 2 sessions (1 year) before submitting a Postgraduate Grant Scheme grant application again.

Students whose application was rejected in one session can apply again after the notification deadline of the rejected grant application

Application Form

- Research Proposal (max. 750 words)
- Title: ....
- Introduction (max. 250 words): .....

Introduce briefly the subject of your PhD and provide relevant background information; summarise previous work by you or others (provide max. 5 relevant references, to be detailed in the 'Bibliography' field). Provide the context for your PhD study in terms of geography, geology, and/or scientific discipline.

- Proposal (max. 250 words): ...

Describe clearly your research proposal and indicate in what way your proposal will contribute to the successful achievement of your PhD. Your application should have a clearly written hypothesis or a well-explained research problem of geologic significance. It should explain why it is important. Simply collecting data without an objective is not considered wise use of resources.

- Methods (max. 125 words): ....

Outline the research strategy (methods) that you plan to use to solve the problem in the field and/or in the laboratory. Please include information on data collection, data analyses, and data interpretation. Justify why you need to undertake this research.

- Facilities (max. 125 words): ....

Briefly list research and study facilities available to you, such as field and laboratory equipment, computers, library.

- Bibliography (max. 125 words)

Provide a list of 5 key publications that are relevant to your proposed research, listed in your 'Introduction'. The list should show that you have done adequate background research on your project and are assured that your methodology is solid and the project has not been done already. Limit your bibliography to the essential references. Each publication should be preceded by a '*'-character (e.g. *Surlyk et al., Sedimentology 42, 323-354, 1995).

- Budget (max. 125 words)

Provide a brief summary of the total cost of the research. Clearly indicate the amount (in Euro) being requested. State specifically what the IAS grant funds will be used for. Please list only expenses to be covered by the IAS grant. The IAS will support field activities (to collect data and samples, etc.) and laboratory activities/analyses. Laboratory activities/ analyses that consist of training by performing the activities/analyses yourself will be considered a plus for your application as they will contribute to your formation and to the capacity building of your home institution. In this case, the agreement of the Head of your Guest Department/Laboratory will be solicited by automated e-mail.

- Curriculum Vitae (max. 250 words)

Name, postal address, e-mail address, university education (degrees & dates), work experience, awards and scholarships (max. 5, considered to be representative), independent research projects, citations of your abstracts and publications (max. 5, considered to be representative).

- Advise of Supervisor and Head of Guest Department/Laboratory

The recommendation letter from the supervisor should provide an evaluation of the capability of the applicant to carry out the proposed research, the significance and necessity of the research, and reasonableness of the budget request. The recommendation letter must be uploaded by the applicant together with the rest of the application content. Applications without letter of support will be rejected. It will be considered as a plus for your application if your PhD supervisor is also a member of IAS.

If you apply for laboratory analyses/activities, please carefully check analysis prices and compare charges of various academic and private laboratories as prices per unit might differ considerably. Please first check whether analyses can be performed within your own University. If your University is not in a position to provide you with the adequate analysis tools, visiting another lab to conduct the analyses yourself strengthens your application considerably as it contributes to your formation and to capacity building of your home University. Please check with the Head of Department/Laboratory of your guest lab to assure its assistance during your visit. You should add a letter of support from him/her with your application.

Finally, before submitting your application, you will be asked to answer a few informative questions by ticking the appropriate boxes.

- is your supervisor a member of IAS
- was this application your own initiative
- did you discuss your application with your Supervisor
- did you already have contact in the past with the Head of the Guest Department/Laboratory (if appropriate)

FOR THE 2ND SESSIONS 2015 THE FOLLOWING STUDENTS ARE GRANTED WITH 1000 EUROS:

NAMES	*UNIVERSITY*	*ALLOCATED*
Yarlett Robert	University of Exeter, UK	ry237@exeter.ac.uk
Boes Evelien	Ghent University, Belgium	Evelien.Boes@UGent.be
Cornacchia Irene	"Sapienza" University of Rome, Italy	irene.cornacchia@uniroma1.it
Dutton Kirsten	Newcastle University, UK	K.E.Dutton1@ncl.ac.uk
Vieten Rolf-Martin	University of Puerto Rico, Mayaguez, Puerto Rico	rolf-martin.vieten@upr.edu
Garberoglio Ricardo	University of Buenos Aires, Argentina	rmg@gl.fcen.uba.ar
Bandyopadhyay Sujay	Indian Institute of Technology Bombay, Mumbai, India	beasiitb@gmail.com
Hashemi Azizi S. Halimeh	University of Hormozgan, Iran	hashemi.azizi@gmail.com
Cipriani Angelo	"Sapienza" University of Rome, Italy	angelo.cipriani@uniroma1.it
Sardar Abadi Mehrdad	Université de Liège, Belgium	Mehrdad.SardarAbadi@student.ulg.ac.be

CALENDAR

EGU 2016 General Assembly*

17th - 22th April 2016
Vienna
Austria

http://egu2016.eu/home.html

1st IMERP-XIV EJIP
(1st International Meeting of Early-stage Researchers in Palaeontology)

13-16 April 2016
Alpuente
Valencia
Spain

1stimerp.xivejip@gmail.com

Conference/Workshop on «Forward Modelling of Sedimentary Systems»*

25th-28th April 2016
Trondheim
Norway

http://www.eage.org/event/index.php?eventid=1415

RCMNS Interim Colloquium «Lake - Basin - Evolution»

19th - 23th May 2016
Zagreb
Croatia

Oleg Mandic
oleg.mandic@NHM-WIEN.AC.AT

32nd IAS Meeting of Sedimentology*

23rd - 25th May 2016
Marrakech
Morocco

32IAS@ibnbattutacentre.org
Ibn Battuta Centre
https://www.sedimentologists.org/ims2016

35th International Geological Congress*

27th August - 4th September 2016
Cape Town
South Africa

http://www.35igc.org/

Siberian Early Career GeoScientists Conference*

13th - 24th June 2016
Akademgorodok, Novosibirsk, Russia

Marianna I Tuchkova
tuchkova@ginras.ru

International Maar Conference*

28 July - 6 August 2016
Changchun City
NE China

Karoly Nemeth
K.Nemeth@massey.ac.nz
http://imc.csp.escience.cn/dct/page/1

Italian Geological Society 88th Congress*

7-9 Sptember
2016
Napoli
Italy

Mariano Parente
Mariano.parente@unina.it
http://www.sginapoli2016.it/

XV Argentinian Meeting of Sedimentology (XV RAS) and VII Latin American Congress of Sedimentology (VII CLS)*

20-23 September
2016
Santa Rosa
Argentina

Adriana Mehl
adrianamehl@gmail.com
xvras2016@gmail.com
http://aasnoticias.blogspot.be/2015/03/xv-reunion-argentina-de-sedimentologia.html

---

XV Reunión Argentina de Sedimentología

September
2016
Santa Rosa, La Pampa
Argentina

Adriana Mehl
adrianamehl@gmail.com
xvras2016@gmail.com

*** THESE EVENTS HAVE FULL OR PARTIAL IAS SPONSORSHIP**

This Newsletter has been designed by
Proedex s.l. Francisco Silvela 27
28028 Madrid, Spain editorial@proedex.com

Contributions to be sent to:
Vincenzo Pascucci
IAS General Secretary
Department of Architecture,
Design and Planning,
University of Sassari,
sede di Via Piandanna 4,
07100 Sassari, Italy
Tel.: +39 079228685
pascucci@uniss.it

IAS

INTERNATIONAL ASSOCIATION OF SEDIMENTOLOGISTS

www.sedimentologists.org